

TECHNICAL UNIVERSITY OF CRETE
SCHOOL OF MINERAL RESOURCES ENGINEERING
MSc in Petroleum Engineering

Reliability of Equilibrium Coefficients Predicting Methods

MSc Thesis

Nodaras C. Efastathios
Mineral Resources Engineer

Supervisor: Prof. Nikolaos Varotsis

Scientific advisor: Dr. Vassilios Gaganis

Chania 2017

ABSTRACT

Equilibrium coefficients (k-values) play a fundamental role in describing and understanding the phase behavior of reservoir fluids either inside the reservoir or on their way to the surface facilities. They correspond to the ratios that the concentration of each component in the vapor and in the liquid phase should exhibit so as to ensure thermodynamic equilibrium. The goal of this study is the evaluation of various k-values estimation methods at several pressures and temperatures against experimental data which has been obtained from several fluid samples.

For this purpose, a PVT experiments data-base is utilized to provide the necessary data for the estimation of k-values at several conditions. The data-base contains data collected through a set of surface flash expansions and differential liberation studies. Furthermore, k-values are estimated from the application of the correlations of Standing (1979) and Wilson (1968) at the same conditions and the results are compared while further taking into account the range of application.

More specifically the behavior of the k-values of light, intermediate and heavy components is examined as the pressure increases by means of charts and it is compared to the typical, theoretically derived k-values curves.

In general good agreement is observed in the results between the two approaches at relatively low pressures, which are pressures encountered at surface facilities rather than the reservoir itself. When the pressure exhibits higher values a deviation of the results of both methods in relation to the experimental k-values is observed.

CONTENTS

| | |
|-------------------------------------------------------------------------------------------|----|
| 1. INTRODUCTION..... | 1 |
| 2. K-VALUES..... | 3 |
| 2.1 EQUILIBRIUM RATIOS..... | 3 |
| 2.2 MATERIAL BALANCE CALCULATIONS CORELATED IN K-VALUES [1] [3] | 5 |
| 2.3 HOFFMAN'S METHOD FOR K-VALUE ESTIMATION..... | 7 |
| 2.4 WILSON'S CORRELATION FOR K-VALUE ESTIMATION..... | 8 |
| 2.5 STANDING'S CORRELATION FOR K-VALUE ESTIMATION [3]..... | 8 |
| 2.6 APPLICATIONS OF K-VALUES..... | 9 |
| 2.6.1 DEW-POINT PRESSURE DETERMINATION..... | 9 |
| 2.6.2 BUBBLE-POINT PRESSURE DETERMINATION..... | 10 |
| 3. PVT TESTS..... | 11 |
| 3.1 SAMPLING..... | 11 |
| 3.1.1 SURFACE SAMPLING..... | 11 |
| 3.1.2 BOTTOM-HOLE SAMPLING..... | 12 |
| 3.2 COMPOSITIONAL ANALYSIS..... | 13 |
| 3.3 OIL & GAS-CONDENSATE PVT TESTS..... | 14 |
| 3.4 MULTISTAGE SEPARATOR TESTS..... | 15 |
| 3.5 DIFFERENTIAL LIBERATION EXPANSION..... | 16 |
| 3.6 CONSTANT COMPOSITION EXPANSION..... | 17 |
| 3.6.1 OIL SAMPLES..... | 17 |
| 3.6.2 GAS CONDENSATE SAMPLES..... | 18 |
| 3.7 CONSTANT VOLUME DEPLETION..... | 18 |
| 4. DATA PROCESSING AND ANALYSIS..... | 21 |
| 4.1 PVT DATA BASE..... | 21 |
| 4.2 K-VALUES OBTAINED FROM SINGLE STAGE FLASH LIBERATION OF BHS..... | 22 |
| 4.3 K-VALUES OBTAINED FROM STOCK TANK OIL AND GAS OF RECOMBINED RESERVOIR SAMPLES..... | 23 |
| 4.4 K-VALUES OBTAINED FROM SEPARATOR OIL AND GAS OF RECOMBINED SAMPLES..... | 23 |

| | |
|-----------------------------------------------------------------------------------------|----|
| 4.5 K-VALUES OBTAINED AT ANY PRESSURE STEPS OF DIFFERENTIAL LIBERATION EXPANSION. | 24 |
| 5. RESULTS AND OBSERVATIONS. | 28 |
| 5.1 K-VALUES OBTAINED FROM SINGLE STAGE FLASH LIBERATION OF BHS. | 28 |
| 5.2 K-VALUES OBTAINED FROM STOCK TANK OIL AND GAS OF RECOMBINED RESERVOIR SAMPLES. | 29 |
| 5.3 K-VALUES OBTAINED FROM SEPARATOR OIL AND GAS OF RECOMBINED SAMPLES. | 31 |
| 5.4 K-VALUES OBTAINED AT ANY PRESSURE STEPS OF DIFFERENTIAL LIBERATION EXPANSION. | 40 |

TABLE OF FIGURES

| | |
|-----------------------------------------------------------------------------------------------------------|----|
| Figure 1: General behavior of a K-value vs. pressure on log-log scale [3]. | 5 |
| Figure 2: Pressure dependence of slope A_1 and intercept A_0 in Hoffman et al. Kp-F relationship [3]. | 7 |
| Figure 3: Surface sampling of oil and gas [3]. | 12 |
| Figure 4: Procedure of recombining single stage separator samples [1]. | 13 |
| Figure 5: Gas chromatograph for compositional analysis of reservoir fluids [3]. | 13 |
| Figure 6: Typical chromatogram for analyzing hydrocarbon composition [3]. | 14 |
| Figure 7: Schematic of a multistage separator test [1]. | 15 |
| Figure 8: schematic of DLE experiment [1]. | 17 |
| Figure 9: schematic of a CCE experiment for oil and a gas condensate [1]. | 18 |
| Figure 10: Schematic of CVD experiment [1]. | 19 |
| Figure 11: Frequency diagram of molar masses of BHS. | 28 |
| Figure 12: Wilson K-values at atmospheric conditions. | 28 |
| Figure 13: K-values of BHS at atmospheric pressure and temperature. | 29 |
| Figure 14: Frequency diagram of molar masses of RSS. | 30 |
| Figure 15: K-values of RSS at atmospheric pressure and temperature. | 30 |
| Figure 16: Frequency diagram of separator pressures. | 31 |
| Figure 17: Frequency diagram of separator temperatures. | 31 |
| Figure 18: Experimental K-values of CH_4 vs. Pressure. | 32 |
| Figure 19: CH_4 Standing's K-values vs. CH_4 Wilson K-values. | 33 |
| Figure 20: K-Values of CH_4 vs. Pressure. | 33 |
| Figure 21: Experimental K-values of C_2H_6 vs. Pressure. | 34 |
| Figure 22: C_2H_6 Standing's K-values vs. C_2H_6 Wilson K-values. | 34 |
| Figure 23: K-Values of C_2H_6 vs. Pressure. | 35 |
| Figure 24: Experimental K-values of C_3H_8 vs. Pressure. | 35 |
| Figure 25: Standing's C_3H_8 K-values vs. Wilson K-values. | 36 |
| Figure 26: K-Values of C_3H_8 vs. Pressure. | 36 |
| Figure 27: Experimental K-values of C_4H_{10} vs. Pressure. | 37 |
| Figure 28: C_4H_{10} Standing's K-values vs. C_4H_{10} Wilson K-values. | 37 |
| Figure 29: K-Values of C_4H_{10} vs. Pressure. | 38 |
| Figure 30: Experimental K-values of C_8H_{18} vs. Pressure. | 38 |
| Figure 31: C_8H_{18} Standing's K-values vs. C_8H_{18} Wilson K-values. | 39 |
| Figure 32: K-Values of C_8H_{18} vs. Pressure. | 39 |
| Figure 33: Frequency diagram of temperatures of Differential Liberation Expansion experiment. | 40 |
| Figure 34 : Frequency diagram of reservoir fluid samples saturation pressure. | 40 |
| Figure 35: Frequency diagram of the reservoir fluid (DLE experiment submitted) molar masses. | 41 |
| Figure 36: Experimental K-values of CH_4 versus Standing's K-values of CH_4 at P_1 . | 41 |

| | |
|-----------------------------------------------------------------------------------------------------------------|----|
| Figure 37: Experimental K-values of C_2H_6 versus Standing's K-values of C_2H_6 at P_1 | 42 |
| Figure 38: Experimental K-values of C_3H_8 versus Standing's K-values of C_3H_8 at P_1 | 42 |
| Figure 39: Experimental K-values of C_4H_{10} versus Standing's K-values of C_4H_{10} at P_1 | 42 |
| Figure 40: Experimental K-values of C_6H_{12} versus Standing's K-values of C_6H_{12} at P_1 | 43 |
| Figure 41: Experimental K-values of C_8H_{14} versus Standing's K-values of C_8H_{14} at P_1 | 43 |
| Figure 42: C_8H_{14} concentration of equilibrium gas and liquid phase at P_1 and reservoir fluid. | 44 |
| Figure 43: Standing's K-values versus Pressure at P_1 | 44 |
| Figure 44: Experimental K-values of CH_4 versus Standing's K-values of CH_4 at P_3 | 45 |
| Figure 45: Experimental K-values of C_2H_6 versus Standing's K-values of C_2H_6 at P_3 | 45 |
| Figure 46: Experimental K-values of C_3H_8 versus Standing's K-values of C_3H_8 at P_3 | 46 |
| Figure 47: Experimental K-values of C_4H_{10} versus Standing's K-values of C_4H_{10} at P_3 | 46 |
| Figure 48: Experimental K-values of C_6H_{12} versus Standing's K-values of C_6H_{12} at P_3 | 46 |
| Figure 49: Experimental K-values of C_8H_{14} versus Standing's K-values of C_8H_{14} at P_3 | 47 |
| Figure 50: Standing's K-values versus Pressure at P_3 | 47 |
| Figure 51: Experimental K-values of CH_4 versus Standing's K-values of CH_4 at P_5 | 48 |
| Figure 52: Experimental K-values of C_2H_6 versus Standing's K-values of C_2H_6 at P_5 | 48 |
| Figure 53: Experimental K-values of C_3H_8 versus Standing's K-values of C_3H_8 at P_5 | 49 |
| Figure 54: Experimental K-values of C_4H_{10} versus Standing's K-values of C_4H_{10} at P_5 | 49 |
| Figure 55: Experimental K-values of C_6H_{12} versus Standing's K-values of C_6H_{12} at P_5 | 49 |
| Figure 56: Experimental K-values of C_8H_{14} versus Standing's K-values of C_8H_{14} at P_5 | 50 |
| Figure 57: Standing's K-values versus Pressure at P_5 | 50 |

1. INTRODUCTION

Each hydrocarbon mixture which is not a single phase one is composed of two phases that coexist in equilibrium at a specific pressure and temperature; these are the gas-phase and the liquid-phase. The equilibrium ratio represents the relation between the quantity of a mixture component which is in the gas-phase and the quantity of the same component that is in the liquid-phase. The Equilibrium ratio or K-value of a component is estimated by the division of component's equilibrium concentration in the gas phase to the component's equilibrium concentration in the liquid-phase. This ratio is differentiated as conditions change. It is obvious that K-values are high-depended on pressure temperature and composition.

K-values are very important for the understanding and the description of the phase behavior petroleum reservoir fluids. This behavior has to be determined for a successful reservoir simulation to be achieved and reliable production and surface processing design to be done. Direct estimation of the K-values at several pressures and temperatures, without the submission of the reservoir fluid sample into PVT tests (pressure, volume, temperature) is a great benefit concerning time and expenses. For this reason many researchers, starting from Katz and Hoffman back in 1950's, have studied the K-values and have implemented correlations and methods for straight forward estimation. In this study the correlations that have been evaluated against experimentally derived K-values are the Standing's, Hoffman's and Wilson's correlation. The basis of this study is a PVT Data-base and the experimental K-values coming from data (gas and liquid phase compositions) that have been measured as the experimental procedure of PVT tests was evolved.

In **Chapter 2** K-values are extensively analyzed as well as their applications. Additionally the correlations and methods of Hoffman's, Standing's and Wilson's are described in detail.

The experimental procedures that provide the necessary data for the extrapolation of the K-values are presented in **Chapter 3**. Initially the sampling procedure and the compositional analysis are described. The PVT tests that are analyzed for oil and gas condensate samples are the Constant Composition Expansion (CCE), Differential Liberation Expansion (DLE), Constant Volume Depletion (CVD) and separator tests.

A PVT data base that contains properties and compositions of almost 900 samples is used for this study. Initially in **Chapter 4** the content of the data base is described. Afterwards the procedure of the implementation of the aforementioned correlations for several cases is analyzed. Experimental and correlation originated K-values have been estimated for single phase flash liberation, stock tank oil and gas, separator oil and gas and for several pressure steps of DLE.

The results as well as the conclusions of this study are presented in **Chapter 5**. The comparison of the K-values resulting by experimental data and correlations is done by plots that describing their behavior at different pressures. Standing's and Wilson K-values are compared between them and also with the experimental K-values and they are evaluated.

2. K-VALUES

Phase equilibrium plays a fundamental role in understanding the phase behavior of hydrocarbon mixtures. Hydrocarbon mixtures consist mainly of two phases, hydrocarbon liquid and hydrocarbon gas. Each phase is characterized by its own physical and chemical properties. The equilibrium ratio between these two phases depends on the constancy of its major variables that involve the system pressure, temperature and overall composition. Equilibrium ratios can be used to describe the phase behavior of petroleum reservoir fluids during primary depletion calculations and in secondary recovery operations such as gas cycling, miscible flooding and thermal methods. The performance of gas-liquid surface separation equipment and separation process in natural gas plants and refineries are predicted by using these ratios. In particular, they are critical for reliable and successful compositional reservoir simulation [2].

2.1 EQUILIBRIUM RATIOS

Equilibrium ratio K-value is defined as the ratio of the component's concentration to the total gas phase composition to the component's concentration to the total liquid phase composition. These two phases have to coexist into equilibrium at a specific pressure and temperature. In other words the K_i is defined as the ratio of equilibrium gas composition Y_i to the equilibrium liquid composition X_i ,

$$K_i = \frac{y_i}{x_i} \quad (2.1)$$

As mentioned before K_i is a function of pressure, temperature and overall composition. K values can be estimated with empirical correlations or by satisfying the equal fugacity constraint with an EOS

$$f_{Li} = f_{vi} \quad i = 1, \dots, N. \quad (2.2)$$

Where f_{Li} is the liquid phase fugacity and f_{vi} is the vapor phase fugacity. Empirical K-value correlations, that are further analyzed below, are useful for reservoir engineering calculations like multistage separation, differential liberation expansion, constant composition expansion (CCE), depletion studies (CVD tests), and for checking the consistency of separator oil gas compositions. Most of the correlations are based on two limiting conditions that show that K-values are high-dependent on the pressure. Rault's and Dalton's laws combination is the first limiting condition at low pressures [3]. Rault's law defines that the partial pressure of a component P_i , in a multi-component system, is the product of its mole fraction in the liquid phase x_i and the vapor pressure of this component p_{vi} at the system temperature

$$p_i = x_i \cdot p_{vi} \quad (2.3)$$

Dalton's law defines that the partial pressure of a component is the product of its mole fraction in the gas phase y_i and the system pressure

$$p_i = y_i \cdot p \quad (2.4)$$

Partial pressures of a component at liquid and gas phase have to be equal at equilibrium so

$$x_i \cdot p_{vi} = y_i \cdot p \quad (2.5)$$

By simple modification of the last equation results the equilibrium ratio of a component K_i at the system pressure p and temperature T_s

$$K_i = p_{vi}(T_s) / p \quad (2.6)$$

This equation involves ideal solutions and the temperature of the system has to be less than the component critical temperature in order for the component vapor pressure to be defined. Also, the equation implies that the K-value is independent of overall composition [1].

The second limiting condition is that, as the pressure increases and the temperature remains constant, the K-values of all components in a mixture tend to converge to 1 at the same pressure. This specific pressure is the convergence pressure. This means that the composition of gas and liquid phase of a component should be the same [4]. In terms of a binary the convergence pressure also represents the critical pressure of the mixture. On the other hand for a multi-component mixture the convergence pressure can not actually exist because the mixture becomes a single phase one at the bubble-point or dew-point pressure, which is a pressure lower than the convergence one. Convergence pressure is a function of overall mixture composition and temperature. The convergence pressure is different for the same mixture at different temperatures. Whitson and Michelsen suggested that convergence pressure has the characteristics of a critical point of a true mixture and can be predicted by an EOS. Rzasa et al. suggested a correlation that is a function of temperature and the product of C_{7+} molecular weight and specific gravity. Standing suggested that convergence pressure of reservoir fluid varies almost linearly with C_{7+} molecular weight [3].

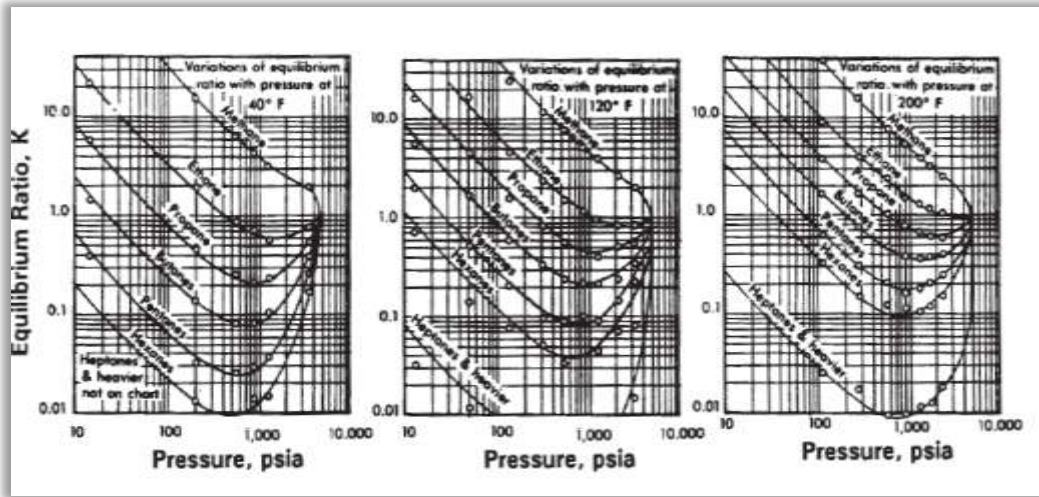


Figure 1: General behavior of a K-value vs. pressure on log-log scale [3].

As shown in the above diagrams that deal with light components ($T > T_c$), K-values decrease monotonically toward the convergence pressure. Heavier components ($T < T_c$) K-values initially decrease due the pressure dependence and pass through unity as the pressure system equals the components vapor pressure. As the pressure further increases comes K-value's minimum and finally an increase occurs up to the unity when the pressure reaches the convergence pressure. The fact is that the minimum pressure of K-values is usually at pressures lower than 1000 psi, reinforces the fact that K-values are almost independent of convergence pressure at low pressures [3].

2.2 MATERIAL BALANCE CALCULATIONS CORELATED IN K-VALUES [1] [3]

Following, Rachford-Rice Procedure for two-phase split calculation will be presented. The initial feed distributes into vapor and liquid phase. As it is stated from the material balance constraints, total number of moles of a hydrocarbon mixture n is equal to the total number of moles in liquid phase n_L and total number of moles in the vapor phase n_V .

$$n = n_V + n_L \quad (2.7)$$

Also total number of moles of a specific component equals to total number of moles of this component in the vapor phase added to the total number of moles of this component in the liquid phase.

$$nz_i = n_V y_i + n_L x_i \quad i = 1, \dots, N. \quad (2.8)$$

Where z_i, y_i, x_i are the mole fraction of the component i in the initial mixture, vapor phase and liquid phase respectively. All the calculations are performed on the basis of one mole so

$$n_L + n_V = 1 \quad (2.9)$$

$$z_i = n_V y_i + n_L x_i \quad (2.10)$$

By the definition of equilibrium ratio

$$K_i = \frac{y_i}{x_i} \quad (2.11)$$

$$y_i = x_i K_i \quad (2.12)$$

$$x_i = \frac{y_i}{K_i} \quad (2.13)$$

So by introducing the equilibrium ratio to the 2.8 equation occurs

$$z_i = n_V (x_i K_i) + n_L x_i \quad (2.14)$$

$$x_i = \frac{z_i}{n_L + n_V K_i} \quad (2.15)$$

$$y_i = \frac{z_i K_i}{n_L + n_V K_i} \quad (2.16)$$

Additionally, the mole fractions of equilibrium phases and the overall mixture must sum to unity.

$$\sum_{i=1}^N y_i = \sum_{i=1}^N x_i = \sum_{i=1}^N z_i = 1 \quad \text{Or} \quad \sum_{i=1}^N (y_i - x_i) = 0 \quad (2.17)$$

$$\sum_{i=1}^N \frac{z_i K_i}{n_L + n_V K_i} - \sum_{i=1}^N \frac{z_i}{n_L + n_V K_i} = 0 \quad (2.18)$$

$$\sum_{i=1}^N \frac{z_i (K_i - 1)}{n_L + n_V K_i} = 0 \quad (2.19)$$

By replacing the n_L with $(1-n_V)$ results

$$\sum_{i=1}^N \frac{z_i (K_i - 1)}{1 + n_V (K_i - 1)} = 0 \quad (2.20)$$

If the feed composition and K-values are known equation 2.20 can be solved in terms of the number of mole being in the vapor phase.

2.3 HOFFMAN'S METHOD FOR K-VALUE ESTIMATION

Hoffman et al. (1953) proposed a method for determination of the K-values but also for checking the consistency of measured K-values.

$$K_i = \frac{10^{(A_0 + A_1 F_i)}}{p} \quad (2.21)$$

$$\log K_i p = A_0 + A_1 F_i \quad (2.22)$$

$$F_i = \frac{1/T_{bi} - 1/T}{1/T_{bi} - 1/T_{ci}} \log(p_{ci}/p_{sc}) \quad (2.23)$$

Where T_c =component critical temperature, p_c =component critical pressure, T_b =component normal boiling point, T =system temperature, p_{sc} =pressure at standard conditions, A_0 and A_1 are the slope and intercept respectively of the plot $\log(K_i p)$ vs. characterization factor F_i .

The basis of this method is that by plotting the logarithm of the equilibrium ratio times the system absolute pressure ($\log K_i p$) vs. the characterization factor F_i , which is mentioned above, occurs a trend that is linear for components C_1 to C_6 at all pressures. The function turns downward for heavier components at low pressures. The trend becomes more linear for all the components at higher pressures. As the pressure increases and reaching the convergence one, K-values tend to unity. That means that $A_0 = \log(p_k)$ and A_1 tend to 0. It is mentioned that plots of ($\log K_i p$) vs. the characterization factor F_i tend to converge at a common point as it is shown to the Figure 2 [3].

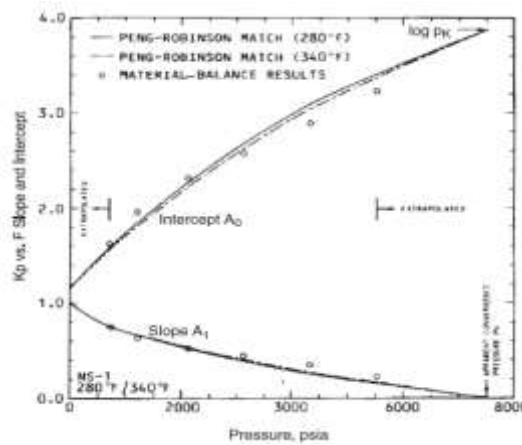


Figure 2: Pressure dependence of slope A_1 and intercept A_0 in Hoffman et al. K_p - F relationship [3].

2.4 WILSON'S CORRELATION FOR K-VALUE ESTIMATION

The equation that follows has been proposed from Wilson in 1968 and is a simplified thermodynamic expression for K-values estimation at low pressures [1].

$$K_i = \frac{\exp 5,37(1 + \omega_i)(1 - T_{ri}^{-1})}{P_{ri}} \quad (2.24)$$

$$P_{ri} = \frac{p}{P_{ci}} \quad T_{ri} = \frac{T}{T_{ci}} \quad (2.25)$$

Where p_{ci} is the critical pressure of the component, p is system pressure, T_{ci} is the critical temperature of component, T is the system temperature, ω_i is the acentric factor of the component. Wilson's equation is identical to the Hoffman's relation for $A_0 = \log(p_{sc})$ and $A_1 = 1$ [3].

Wilson's equation has been reformulated by Whitson and Torp (1981). The equation was modified, in terms of acentric factor and convergence pressure p_K , so to produce accurate results at higher pressures [1].

$$K_i = \left(\frac{P_{ci}}{P_K} \right)^{A_1 - 1} \frac{\exp \left[5,37 A_1 (1 + \omega_i) (1 - T_{ri}^{-1}) \right]}{P_{ri}} \quad (2.26)$$

A_1 is a function of pressure. When pressure reaches the convergence pressure $P = P_K$ then $A_1 = 0$, when $P = P_{sc}$ then $A_1 = 1$.

$$A_1 = 1 - \left(\frac{P}{P_K} \right)^{A_2} \quad (2.27)$$

A_2 ranges from 0.5 to 0.8 [3].

2.5 STANDING'S CORRELATION FOR K-VALUE ESTIMATION [3]

Standing's correlation is based on Hoffman method and is modified to generate a low-pressure ($P < 1000$ psi, $T < 200^\circ$ F) K-value equation for surface calculations.

$$K_i = \frac{10^{(A_0 + A_1 F_i)}}{p} \quad (2.28)$$

$$F_i = b_i \left(\frac{1}{T_{bi}} + \frac{1}{T} \right) \quad (2.29)$$

$$b_i = \log(p_{ci}/p) / \left(\frac{1}{T_{bi}} + \frac{1}{T_{ci}} \right) \quad (2.30)$$

A_0 and A_1 are functions of pressure based on K-value data from an Oklahoma City crude oil.

$$A_0 = 1,2 + (4,5 \cdot 10^{-4})p + (15 \cdot 10^{-8})p^2 \quad (2.31)$$

$$A_1 = 0,890 - (1,7 \cdot 10^{-4})p - (3,5 \cdot 10^{-8})p^2 \quad (2.32)$$

Standing's low-pressure correlation is significantly useful for checking the consistency of separator gas and oil compositions.

2.6 APPLICATIONS OF K-VALUES

Knowing the equilibrium ratio values of a component of a hydrocarbon mixture at different pressures and temperature is a very important benefit towards solving phase equilibrium problems in reservoir and process engineering [1].

2.6.1 DEW-POINT PRESSURE DETERMINATION

The dew-point pressure is the pressure that the first drop of liquid appears. The material balance equation apply to the saturation pressure, so if all the calculations are performed on the basis of one mole feed (eq.2.9), at this pressure it can be considered that the total number of moles being in the vapor phase equal to unity and the total number of moles being to the liquid phase equal to zero.

$$n_L = 0, \quad n_V = 1 \quad (2.33)$$

Applying the above constraints to the Rachford-Rice equation occurs that

$$\sum_{i=1}^N \frac{z_i(K_i - 1)}{1 + n_V(K_i - 1)} = 0 \rightarrow \sum_{i=1}^N \frac{z_i(K_i - 1)}{K_i} = 0 \rightarrow \sum_{i=1}^N z_i - \sum_{i=1}^N \frac{z_i}{K_i} = 0 \rightarrow$$

$$\sum_{i=1}^N \frac{z_i}{K_i} = 1 \quad (2.34)$$

Using the correlations of K-value estimation, that have already mentioned, the dew-point pressure can be estimated with a trial and error process. The appropriate value of pressure has to be introduced to the correlation, for the right K-value of the component to be estimated, so as the sum (eq. 2.34) to be equal to 1.

2.6.2 BUBBLE-POINT PRESSURE DETERMINATION

When the pressure reaches the bubble point pressure, the first bubble of gas appears. The material balance equation apply to the saturation pressure, so if all the calculations are performed on the basis of one mole feed (eq.2.9), at this pressure it can be considered that the total number of moles being in the vapor phase equal to zero and the total number of moles being to the vapor phase equal to unity.

$$n_L = 1, \quad n_V = 0 \quad (2.35)$$

By applying the above constraints to the Rachford-Rice equation yields

$$\sum_{i=1}^N \frac{z_i(K_i - 1)}{1 + n_V(K_i - 1)} = 0 \rightarrow \sum_{i=1}^N z_i(K_i - 1) = 0 \rightarrow \sum_{i=1}^N z_i K_i - \sum_{i=1}^N z_i = 0 \rightarrow$$
$$\sum_{i=1}^N z_i K_i = 1 \quad (2.36)$$

Equilibrium ratio of a component can be estimated from correlations. The pressure that gives the K-value that satisfies the equation 2.36 is the saturation pressure. A trial and error process have to be done for the bubble-point pressure to be estimated.

BIBLIOGRAPHY

1. Ahmed, T. (1989). Hydrocarbon Phase Behavior. *Gulf, Houston, TX*, 226.
2. Yarborough, L. (1972). Vapor-liquid equilibrium data for multi-component mixtures containing hydrocarbon and non-hydrocarbon components. *Journal of Chemical & Engineering Data*, 17(2), 129–133.
3. Whitson, C. H., & Brule, M. R. (2000). Phase Behavior. SPE Monograph Volume 20 (Vol. 20, p. 233).
4. Danesh, D. (1998). PVT and Phase Behavior of Petroleum Reservoir Fluid, Elsevier.

3. PVT TESTS

The aim of the implementation of the PVT (pressure, volume, temperature) tests is the determination and measuring of volumetric and phase behavior of reservoir fluid, as it travels from the reservoir up to the surface and as the pressure declines with production. In a PVT laboratory researchers are trying to determine accurate oil and gas sample properties and achieve the optimal simulation of the flow in the reservoir, up to the well and through the separators [3]. The laboratory analyses that can be made on a reservoir sample depending on the amount of data that is needed to be determined. In general there are three types of tests [2].

- The primary tests that involve the measurements of specific gravity and gas to oil ratio of the produced fluids.
- Detailed laboratory tests that involve the compositional analysis of the fluid and molecular weight, viscosity, compressibility, saturation pressure, formation volume factor measurements. Also the characteristics that arise from the differential liberation, constant volume depletion and constant composition expansion experiments are reported.
- Swelling is the last type of test and may be performed at special cases that the reservoir is to be depleted under gas injection.

3.1 SAMPLING

For a successful PVT analysis to be done, a representative reservoir fluid sample is needed to be collected. The original reservoir fluid sample has to get analyzed as soon as the exploration wells are drilled up. Characteristics and properties of analyzed fluid sample have to be optimal same to the original reservoir fluid properties. There are two types of samples. The samples can be sampled down-hole or at the surface [3].

3.1.1 SURFACE SAMPLING

At surface sampling reservoir fluids are created from the recombination of separator oil and gas. Separator oil composition is determined by the following steps

- Separator oil sample is flashed to atmospheric conditions.
- Volumes of stock tank oil V_{STO} and gas V_{STG} are measured.
- Weight fractions of stock tank oil W_{STO} and gas W_{STG} are determined by gas chromatography.
- Stock tank oil molecular weight M_o and specific gravity γ_o are measured.
- Weight fractions are normalized to mole fractions X_i and Y_i .
- Separator oil composition is recombined mathematically.

Weight fractions of separator gas occur after its introduction into a gas chromatograph. As is said before weight fractions are converted to mole fractions Y_i . Separator gas specific gravity γ_G is measured and C_{7+} molecular weight is calculated.

A PVT report includes the separator gas/oil ratio R_{SEP} (standard gas volume per separator oil volume) and the separator oil formation volume factor B_{OSEP} (volume of separator oil is needed for 1 barrel of oil in standard condition (STB) to occur).

Well-stream composition Z_i is calculated by the equation (3.1):

$$z_i = n_g y_i + (1 - n_g) x_i \quad (3.1)$$

Where n_g is the mole fraction of well stream mixture that becomes separator gas. Separator compositions can be tested in regard to their consistency using K value estimation correlations like Hoffman et al. and Standing's for low pressures [1]. The advantage of surface sampling is that the procedure of sampling is easier and more beneficial as regards the costs. On the other hand the measurements have to be very accurate so the recombination to be successful [3].

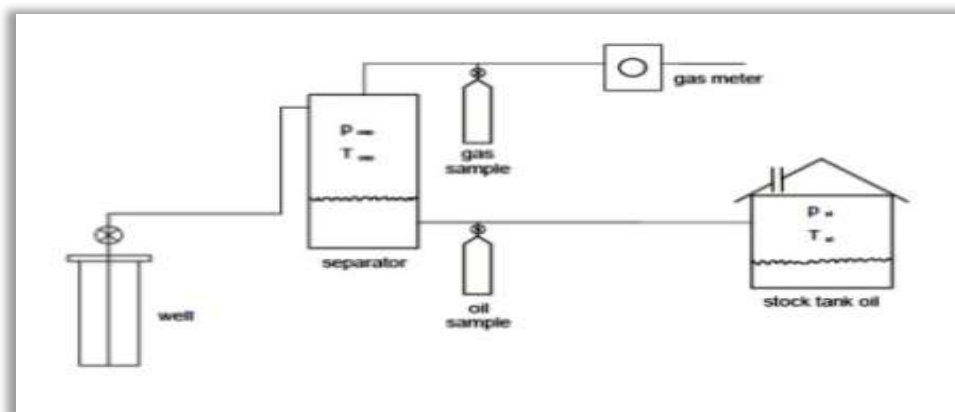


Figure 3: Surface sampling of oil and gas [3].

3.1.2 BOTTOM-HOLE SAMPLING

This kind of sampling requires a bottom-hole sampler that is used combined in a pressure gauge. After the sampler reaches the production zone, the sample chamber is opened and the reservoir fluid flows slowly into the tool at constant pressure. At least three samples have to be collected from the production zone each time. The procedure of composition determination of the bottom-hole sample is same to the separator oil's, which is described in the section 3.2.1 (Figure 3).

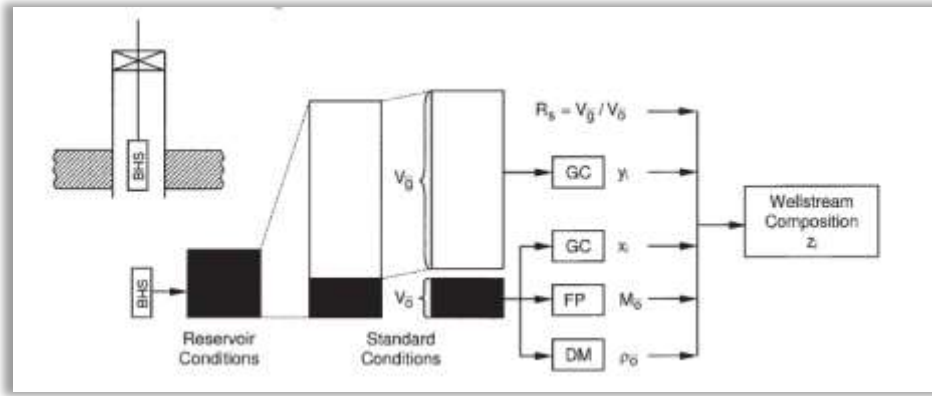


Figure 4: Procedure of recombining single stage separator samples [1].

A successful bottom-hole sampling is needed to be implemented in a stabilized well. This means that the surface gas to oil ratio and pressure are stabilized. Reservoir samples can be saturated or under-saturated, so the treatment of each one is not the same. A conditioned well (pressure drawdown have passed) ensures the similarity of the nature of the fluid traveling up to the wellbore with the reservoir fluid's one. Bottom-hole sample characteristics are first determined in the field and after in the PVT laboratories. Properties of different samples from the same well have to be almost identical [3].

3.2 COMPOSITIONAL ANALYSIS

Reservoir sample's compositional analysis is very important for a successful PVT analysis. The main compositional analysis technique is gas chromatography (GC). GC like distillation is a method of separating the components of a mixture by utilizing their different migration velocities through a column filed with a porous media. In this technique the fluid sample has to be heated up to the point that evaporates and then to be circulated through the columns of porous absorbing media (solid silica gel, charcoal) with the help of a carrier gas.

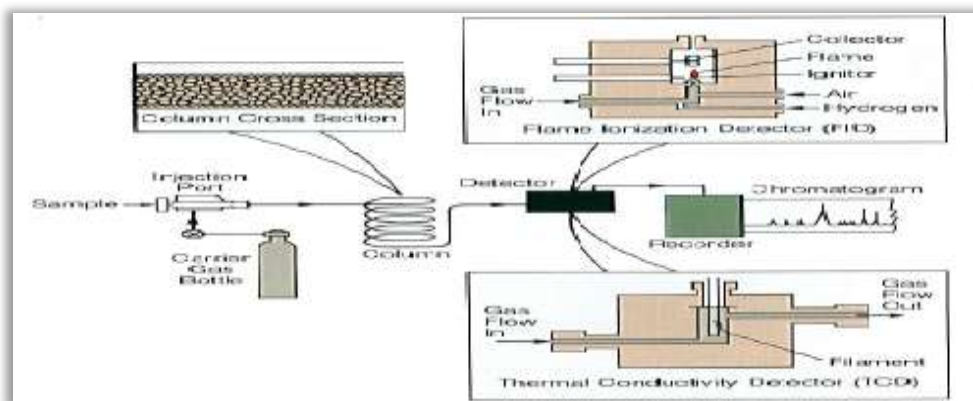


Figure 5: Gas chromatograph for compositional analysis of reservoir fluids [3].

The sample is injected into the injection socket of the chromatograph by a syringe or a gas sampling valve. For the vaporization to be achieved, the sample is heated up to 850 °F (450°C) and an inert carrier gas like helium transports it through the column route. Lighter components pass through the columns faster than the heavier ones due to their differential absorption. This way they are identified. This happens comparing components retention time at the column with known previously analyzed components at the same conditions. After the circulation the compound reaches the detector. There are two types of detectors, the FID (flame ionization detector) and the TCD (thermal conductivity detector). The concentration of each compound is measured by these detectors. The result of the above procedure is a chromatogram and the size of a chromatographic peak is proportional to the amount of component that corresponds to this peak (Figure 6) [3].

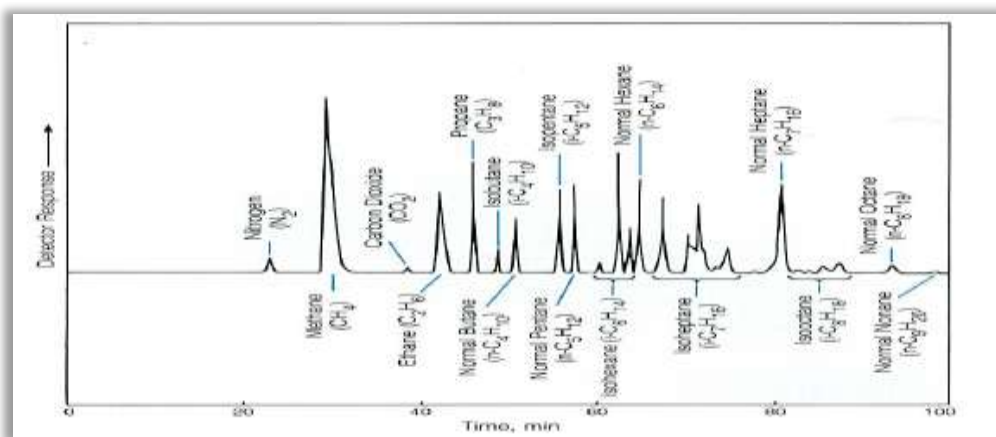


Figure 6: Typical chromatogram for analyzing hydrocarbon composition [3].

The disadvantage of gas chromatography is that high boiling point components cannot be eluted, hence they can't be detected. Depending on the sample nature, an amount of material remains in the column, however this amount has to be accounted for the overall composition to occur. To quantify heavy end, the sum of mass of the eluted components have to be subtracted from the injected mass. Capillary gas chromatography is a more advanced technique and is used to analyze petroleum fluid up to C35+ [2].

3.3 OIL & GAS-CONDENSATE PVT TESTS

Standard PVT Analysis for oils include

- Bottom-hole well-stream compositional analysis.
- Constant composition expansion (CCE).
- Differential liberation expansion (DLE).
- Separator tests.

CCE experiment provides the bubble-point pressure and volumetric properties of under-saturated oil. The DLE and separator test experiment determine black oil properties like oil formation volume factor B_o and gas to oil ratio R_s that are needed for reservoir engineering calculations [1].

Standard PVT Analysis for gas condensates include

- Recombined well-stream compositional analysis.
- Constant composition expansion (CCE).
- Constant volume depletion (CVD).

The CVD and CCE experiments are implemented in high pressure visual cells and the dew-point is determined visually. At CVD experiment the retrograde condensation is being studied by measuring phase volumes at each pressure step [2].

3.4 MULTISTAGE SEPARATOR TESTS

Multistage separator tests are mainly conducted on an oil sample to get information to design and optimize the surface process. Several separator tests are implemented to maximize the production of stock tank oil but also to maximize the concentration of dissolved lighter compounds in the stock tank oil and not in the surface gas [2]. Two or three stages are set, with the first one being at pressure and temperature near to the saturation one and the last one being near or exactly at the tank pressure and temperature. Properties that are measured include initial volume at saturation pressure, separator and stock tank oil and gas volumes at each step, density and composition [1].

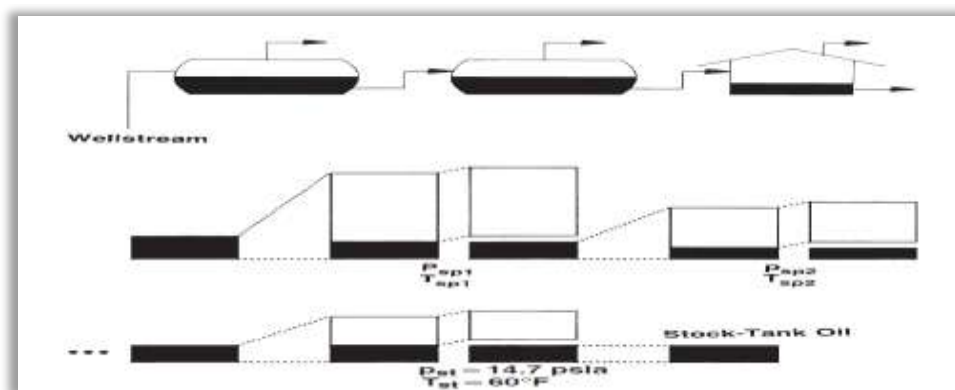


Figure 7: Schematic of a multistage separator test [1].

At first the reservoir sample that could be bottom-hole or recombined is brought to saturation conditions and its volume is measured. Following, it reaches the first-stage separator pressure and temperature. The gas that has been produced is removed and the volume of oil (V_{OSP}) at this stage is recorded. Also the volume (V_g),

the number of moles (n_g), the specific gravity (γ_g) and the composition (y) of removed gas are measured. The remaining oil is brought to the second separator-stage and the same procedure is repeated. As earlier on mentioned, at the final separator-stage the oil is brought to the atmospheric or stock tank conditions. Residual oil's volume and specific gravity are measured. Gas to oil ratio (R_s) is measured at each step and is expressed as gas volume at standard conditions (SCF) per stock tank oil volume (STB) [1].

3.5 DIFFERENTIAL LIBERATION EXPANSION

Differential liberation expansion (DLE) experiment is also called as differential vaporization. This test is carried out on reservoir oils to simulate the depletion process of the reservoir and provide the data that is needed to decode the phase behavior of the fluid as the pressure drops and the gas amount increases.

The reservoir sample is placed single phase in a high-pressure, high-temperature blind cell at reservoir conditions. After that the pressure is lowered with the displacement of the mercury and the sample expands [3]. When the bubble-point pressure is reached the oil volume is recorded. At each pressure step, and following the agitation of the mixture for equilibrium to be achieved, the liberated gas is removed from the cell and proportional amount of mercury is re-injected to reach the previous pressure. The volume, moles and specific gravity of the discharged gas are measured. The remaining oil volume is also recorded. This procedure is repeated 10 to 15 times. Residual oil volume and specific gravity are measured at 60°F [1].

The measured data basis consists of the following:

- Volume of removed gas at each step ΔV_g
- Moles of removed gas at each step Δn_g
- Specific gravity of removed gas at each step γ_g
- Volume of remaining oil at each step V_o
- Volume of stock tank oil V_{or}
- Specific gravity of stock tank oil γ_{or}

Obtained data

- Composition of the liberated gas y_i
- Compressibility factor of the liberated gas Z
- Density of the remaining oil ρ_o
- Gas/Oil ratio of the differential solution R_{sd}
- FVF of the differential oil B_{od}

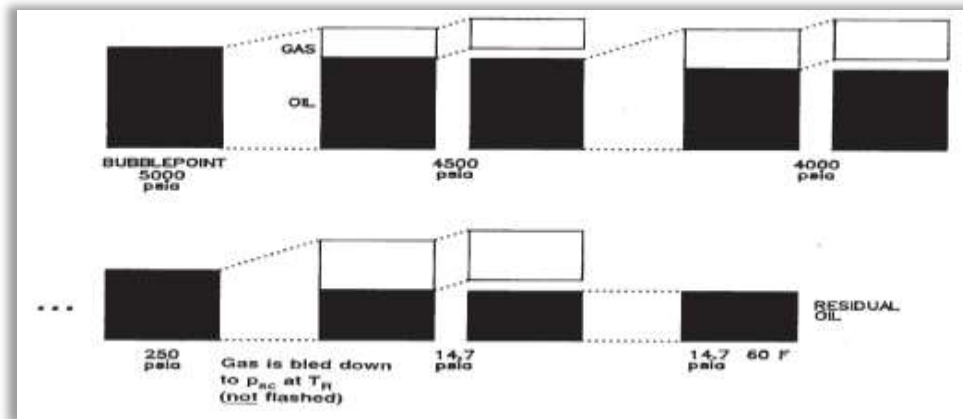


Figure 8: schematic of DLE experiment [1].

Flash liberation is another type of liberation with similar experimental procedure. The difference between DLE and Flash liberation is that a sudden pressure drop causes gas to come out of solution but it remains in contact with remaining oil. It could be said that Flash liberation process simulates the gas liberation and gas behavior at pressures immediately below bubble point pressure. This means that the liberated gas remains immobile and in contact with remaining oil until it reaches the critical gas saturation. As the saturation of the liberated gas reaches the critical gas saturation, it starts to flow separated from the remaining oil. This behavior is proportional to the DLE process [2].

3.6 CONSTANT COMPOSITION EXPANSION

The constant composition expansion (CCE) is a PVT test that can be implemented for both oils and gas condensates. It is also called mass expansion or Flash vaporization.

3.6.1 OIL SAMPLES

This experiment provides bubble point pressure determination, under-saturated oil density, isothermal oil compressibility and two phase volumetric behavior at pressures below bubble-point. Reservoir fluid sample is introduced in a blind cell and the mass of the sample is recorded. Temperature of the experiment is constant and is the reservoir one. The pressure is a bit higher than the reservoir one and the sample is in single phase. The pressure is reduced in steps (5-200psi) at constant temperature by removing mercury from the cell and the expanding hydrocarbon volume is measured at each step. To avoid super-saturation, where the mixture remains single phase even if it should exist in two phases the fluid is agitated by rotating the cell. Below the bubble point the total volume and compressibility of the mixture will get increased, due to the gas liberation from the oil.

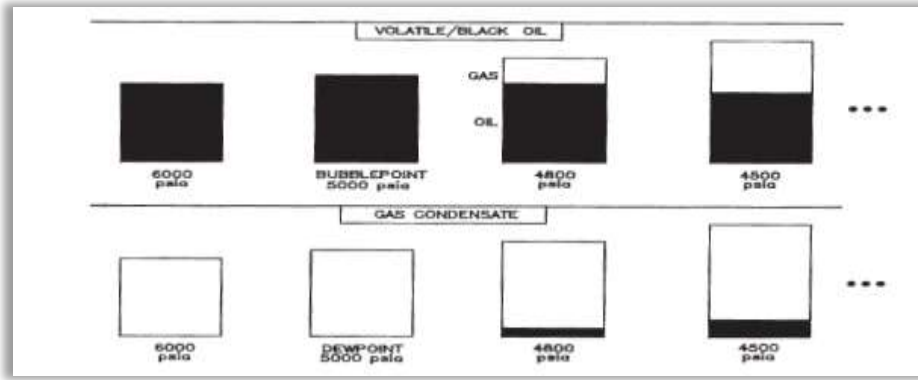


Figure 9: schematic of a CCE experiment for oil and a gas condensate [1].

Recorded cell volumes are plotted versus pressure and the discontinuity in volume at the bubble-point is obvious. For volatile oils the volume discontinuity is not obvious in the P-V curve so a windowed cell is used to visually determine the saturation pressure. The volume at the bubble-point (saturation pressure) is used as a reference. Relative volume of each pressure is recorded as a ratio of the reference volume ($V_r = V/V_{sat}$). Density at the saturation pressure (ρ_{ob}) and compressibility above that are also reported. Isothermal compressibility can be expressed in terms of V_r [1].

$$c = \frac{1}{V_r} \left(\frac{\partial V_r}{\partial P} \right)_T \quad (3.2)$$

3.6.2 GAS CONDENSATE SAMPLES

The procedure that is implemented in gas condensate samples is the same with the oil sample procedure. CCE experiments take place in a visual cell and the data that are provided are: the total relative volume V_{rt} , which is defined as the volume of the mixture or gas divided by the dew-point volume. The deviation factor Z is also provided and is reported at pressures greater than an equal to the saturation pressure. FVF of wet gas is reported at dew point and initial reservoir pressure [1] [2].

3.7 CONSTANT VOLUME DEPLETION

Constant volume depletion tests are implemented in gas condensate samples and rarely in volatile oil samples and provides volumetric and compositional data that could predict and determine the pressure depletion performance of a gas-condensate reservoir. The procedure is described by the Figure 3.8.1. The provided data are

- A reservoir material balance that gives average pressure versus recovery of total well-stream (wet-gas recovery)

- Produced well-stream composition and surface products versus reservoir pressure
- Average oil saturation in the reservoir that occurs during pressure depletion

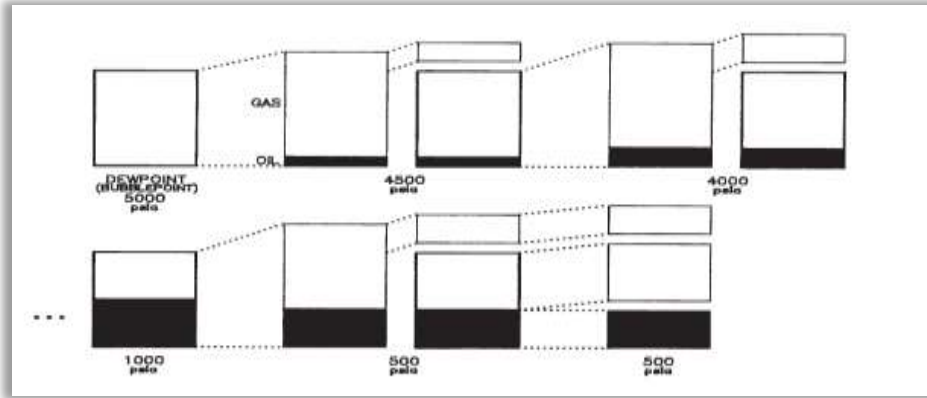


Figure 10: Schematic of CVD experiment [1].

Initially a measured amount of reservoir sample with known composition is injected in a visual cell at the saturation pressure (dew-point pressure) and reservoir temperature. The saturation volume V_i is used as a reference volume [2]. Then the pressure level is decreased, by withdrawing mercury from the cell. This way a second phase (retrograde liquid) is formed. When equilibrium occurs the total volume V_t and volume of retrograde liquid V_l is measured. Retrograde volume is expressed as a percent of the initial volume. The next step is the re-injection of mercury in the cell with proportional amount of gas to be removed at constant pressure. Removed gas and occurring condensate get analyzed and their compositions y_i and x_i are calculated. Also volume ΔV_g and ΔV_o , densities ρ_o and ρ_g and oil molecular weight M_o are measured [1]. Moles of removed gas can be calculated from

$$\Delta n_g = \frac{\Delta V_o \rho_o}{M_o} + \frac{\Delta V_g}{379} \quad (3.3)$$

And equilibrium gas Z factor can be calculated from

$$Z = \frac{p \Delta V_g}{\Delta n_g RT} \quad (3.4)$$

BIBLIOGRAPHY

1. Whitson, C. H., & Brule, M. R. (2000). Phase Behavior. SPE Monograph Volume 20 (Vol. 20, p. 233).

2. Ahmed, T. (1989). Hydrocarbon Phase Behavior. *Gulf, Houston, TX*, 226.
3. The Technical review, volume 37 (January 1989), Schlumberger publication, Varotsis Nikos, Guieze Paul.

4. DATA PROCESSING AND ANALYSIS

In this chapter the K-values extraction process as well the data analysis being performed in the PVT data base will be presented. The data base is an excel-file that contains measured properties of analyzed oil and gas samples. PVT measurements of recombined and bottom-hole samples are included also. All the samples are characterized concerning their origin and they are differentiated according to the experimental procedure that they have undergone. This data base constitutes the feed data for a new excel-file that has been created, for the necessary data analysis to be done and the K-values to be exported. In this way K-values based on experimental data are produced. On the other hand K-values estimation correlations are applied so that their results can be compared to the equilibrium ratios originated from compositional analysis.

4.1 PVT DATA BASE

The given data base contains properties and measurements of about 700 samples. As mentioned before the samples have been characterized, as concerns their fluid type. For the PVT measurements, bottom-hole and recombined reservoir fluid samples are used. The types of fluids are the next and for shortness reasons an ID-number that is mentioned is used:

- [1] Flashed liquid (single stage Flash Liberation) from bottom-hole samples (BHS) or recombined surface samples (RSS).
- [2] Flashed gas (single stage Flash Liberation) from BHS or RSS.
- [3] Reservoir fluid.
- [4] Stock tank liquid (residual oil).
- [5] Stock tank gas.
- [6] Separator liquid.
- [7] Separator gas.
- [8] Gas obtained at each pressure step of Differential Liberation Expansion (DLE).
- [9] Gas obtained at each pressure step of Depletion study (CVD).
- [10] Gas obtained at each pressure step of standalone Separator Tests.

All the above types of fluid could be obtained from one fluid sample that has been submitted to all the necessary experimental procedures (PVT tests). Reservoir fluid sample can be bottom-hole or surface sample. In case that a BHS is provided, it has to be flashed at standard conditions so the flashed liquid [1] and the flashed gas [2] arise. At next compositional analysis of them has to be done by gas chromatography. The last step is the mathematical recombination of the [1] and [2] so that the composition of the reservoir fluid [3] to arise. In case of surface sampling stock tank

liquid [4], stock tank gas [5] and separator gas [7] samples are analyzed. Their composition transpires from analyzing them by gas chromatography. The separator liquid [6] composition is obtained from the mathematical recombination of the stock tank liquid and gas. At next having the composition of separator liquid [6] and gas [7] and by mathematical recombination, the reservoir fluid [3] composition is estimated. It has to be mentioned that separator pressure and temperature are measured and provided.

The oil samples are submitted to DLE tests and at each pressure step the removed gas [8] composition is determined by GC. Also the gas samples are submitted to CVD tests and at each pressure step the removed gas [9] composition is determined by GC. PVT tests have to be done at reservoir temperature and this temperature is provided. Stand alone separator tests are being made to the reservoir fluids for the ideal separation conditions to be determined. Separator gas [10] composition at each pressure step is determined. Separation of lighter fluids is more difficult so more separator tests are needed.

The range of compositional analysis differentiates between the samples. The majority of the samples have been analyzed up to C₁₂. Heavy end's molar mass and density are measured and they are used for the critical properties to be determined. The other pure components properties and critical properties are used as defined by Katz tables. These tables contain properties that have been estimated using true boiling point (TBP) distillation methods.

4.2 K-VALUES OBTAINED FROM SINGLE STAGE FLASH LIBERATION OF BHS.

Bottom-hole samples that had been analyzed through C₁₂ selected for the extrapolation of K-values. The number of them was 265. As mentioned before these samples have been flashed to the atmospheric conditions and flashed gas and liquid occurred. Having the compositions of flashed gas and liquid, the K-value of each component at atmospheric conditions is determined by a simple division. These K-values will be referred as experimental.

Wilson's correlation has been used also for the estimation of K-values. This method has been chosen because is the simplest one and as the pressure is the atmospheric and temperature low, can be applied.

$$K_i = \frac{\exp 5,37(1 + \omega_i)(1 - T_{ri}^{-1})}{p_{ri}} \quad (4.1)$$

$$p_{ri} = \frac{p}{p_{ci}} \quad T_{ri} = \frac{T}{T_{ci}} \quad (4.2)$$

The critical pressure P_c and temperature T_c as well the acentric factor ω are necessary for the estimations. These properties are known for the components through C_{11} . For the heavy end T_{wu} correlations are used for the critical pressure P_c and temperature T_c estimation and Kesler-Lee correlation is used for the acentric factor ω estimation. The needed properties for the application of these correlations are the molecular weight $MW_{C_{12+}}$ and the specific gravity $Sg_{C_{12+}}$ that are provided. The experimental K-values will be compared with the K-values originated from Wilson's correlation at the Chapter 5.

4.3 K-VALUES OBTAINED FROM STOCK TANK OIL AND GAS OF RECOMBINED RESERVOIR SAMPLES.

The procedure of the creation of the initial reservoir fluid by recombination of the separator liquid and gas has already mentioned. In this sub-chapter K-values that occur from the separator liquid flash liberation to stock tank liquid and gas are examined. For this individual study 292 couples of stock tank liquid and gas samples are used. All of them have been analyzed through C_{12} . These samples have been analyzed and their composition is provided. Experimental K-values are estimated by the division of each component's gas concentration to the liquid one.

As the conditions of the flash are the atmospheric and due to its simplicity, the correlation that is selected for the extrapolation of the K-values is the Wilson's. The procedure that is followed and the equations that are used are the same to the one that is described for the K-values obtained from single phase flash liberation of bottom-hole samples. The experimental K-values will be compared with the K-values originated from Wilson's correlation at the next chapter.

4.4 K-VALUES OBTAINED FROM SEPARATOR OIL AND GAS OF RECOMBINED SAMPLES.

Separator gas and oil coexist into equilibrium at the separator pressure and temperature. At these conditions experimental K-values are produced by knowing the composition of each phase. Experimental K-values are estimated by the division of each component's concentration at the gas phase to the liquid phase one. Liquid phase composition is calculated by recombination of flashed liquid and gas. 292 couples of separator liquid and gas samples are examined. All of them have been analyzed through C_{12} .

Wilson's correlation is used for the estimation of K-values at separator conditions. The procedure that is followed and the equations that are used are the same to the previous studies. The only difference is that separator pressure and temperature are introduced to the equation. Wilson's correlation is used by definition at low pressures so it is expected that at high pressure separators the results are going to have a deflection. The experimental K-values will be compared with the K-values originated from Wilson's correlation at the Chapter 5.

Standing's correlation is the last one that is used for the estimation of separator K-values. The majority of the samples are at conditions that the using of this correlation makes sense. The equations that are used are the next:

$$K_i = \frac{10^{(A_0 + A_1 F_i)}}{p} \quad (4.8)$$

$$F_i = b_i \left(\frac{1}{T_{bi}} + \frac{1}{T} \right) \quad (4.9)$$

$$b_i = \log(p_{ci}/p) / \left(\frac{1}{T_{bi}} + \frac{1}{T_{ci}} \right) \quad (4.10)$$

$$A_0 = 1,2 + (4,5 \cdot 10^{-4})p + (15 \cdot 10^{-8})p^2 \quad (4.11)$$

$$A_1 = 0,890 - (1,7 \cdot 10^{-4})p - (3,5 \cdot 10^{-8})p^2 \quad (4.12)$$

Once again component critical temperature T_c , critical pressure p_c and normal boiling point T_b are estimated by Twu correlations. T is the system temperature and P is the system pressure. The experimental K-values will be compared with the K-values originated from Standing's correlation at the Chapter 5.

4.5 K-VALUES OBTAINED AT ANY PRESSURE STEPS OF DIFFERENTIAL LIBERATION EXPANSION.

For this study 188 samples of recombined reservoir fluid were selected. These samples have been bought to the saturation conditions and have been submitted to differential liberation (DL) PVT test at some pressure steps. For all of them, 5 pressure steps bellow the bubble point has been selected. As mentioned before at each pressure step the gas that is removed gets analyzed through GC and its composition is provided. Also, the composition of the initial reservoir fluid has been estimated by recombination of the separator gas and liquid and is provided. For the experimental K-values to be determined the composition of the equilibrium liquid at

each pressure step has to be determined. The procedure and the equations that were used will be presented bellow.

At a DL study the reservoir fluid is depleted isothermally from the bubble point pressure to the atmospheric one at n_{DV} steps. Compositions of equilibrium liquid and gas is set $x^{(i)}$ and $y^{(i)}$ respectively at step i , $1 \leq i \leq n_{DV}$. Composition of reservoir fluid is $x^{(0)}$ and $y^{(0)}$ is the bubble point gas composition which cannot be measured. The solution gas-to-oil ratio $R_s^{(i)}$ is defined by:

$$R_s^{(i)} = \frac{\sum_{k=i+1}^{n_{DV}} N_g^{(k)} \frac{RT_{sc}}{P_{sc}}}{V_o^{(n_{DV}+1)}} \quad (4.13)$$

$N_g^{(k)}$ denotes the moles of liberated gas at step k and $V_o^{(n_{DV}+1)}$ is the volume of the residual oil. The solution gas-to-oil ratio difference between steps i and $i-1$ is:

$$R_s^{(i-1)} - R_s^{(i)} = \frac{\sum_{k=i}^{n_{DV}} N_g^{(k)} \frac{RT_{sc}}{P_{sc}}}{V_o^{(n_{DV})}} - \frac{\sum_{k=i+1}^{n_{DV}} N_g^{(k)} \frac{RT_{sc}}{P_{sc}}}{V_o^{(n_{DV})}} = \frac{N_g^{(i)}}{V_o^{(n_{DV})}} \frac{RT_{sc}}{P_{sc}} \quad (4.14)$$

Gas phase molar ratio at step i is:

$$n_g^{(i)} = \frac{N_g^{(i)}}{N_o^{(i)} + N_g^{(i)}} \Rightarrow \frac{N_g^{(i)}}{N_o^{(i)}} = \frac{n_g^{(i)}}{1 - n_g^{(i)}} \quad (4.15)$$

Residual oil volume and reservoir oil volume at any pressure step are related through B_o :

$$V_o^{(n_{DV})} = \frac{V_o^{(i)}}{B_o^{(i)}} \quad (4.16)$$

The reservoir oil volume is expressed through density as:

$$V_o^{(i)} = \frac{m_o^{(i)}}{\rho_o^{(i)}} = \frac{N_o^{(i)} M_o^{(i)}}{\rho_o^{(i)}} \quad (4.17)$$

By applying a material balance equation, composition of the liquid phase $x^{(i)}$ can be expressed as:

$$x^{(i-1)} = (1 - n_g^{(i)}) x^{(i)} + n_g^{(i)} y^{(i)} \Rightarrow x^{(i)} = \frac{x^{(i-1)} - n_g^{(i)} y^{(i)}}{1 - n_g^{(i)}} \quad (4.18)$$

Reservoir oil molar mass $M_o^{(i)}$ can be expressed as a function of its composition:

$$M_o^{(i)} = \frac{M_o^{(i-1)} - n_g^{(i)} M_g^{(i)} \sum_c y_c^{(i)} MW_{(c)}}{1 - n_g^{(i)}} \quad (4.19)$$

Where

$$M_g^{(i)} = \sum_c y_c^{(i)} MW_{(c)} \quad (4.20)$$

Substituting (4.15) and (4.20) in (4.14) obtain that:

$$n_g^{(i)} = \frac{(R_s^{(i-1)} - R_s^{(i)}) M_o^{(i-1)}}{\frac{RT_{sc}}{p_{sc}} B_o^{(i)} \rho_o^{(i)} + (R_s^{(i-1)} - R_s^{(i)}) M_g^{(i)}} \quad (4.21)$$

Starting from the first pressure step below the bubble point, the molar mass of the gas phase is calculated by the multiplication of the gas composition with the component molar mass as defined by Katz tables. By the same procedure molar mass of the reservoir fluid at the bubble point pressure is determined. Gas phase at saturation pressure considered non-existent. The gas-to-oil ratio R_s , formation volume factor B_o , and the relative oil density ROD have been measured through the DL experiment and an excel-file containing the factors and the implementation of these three properties have been created. The equation (4.21) can be applied and the gas phase molar ratio n_g can be calculated for the first pressure step. The equation (4.18) can be applied and equilibrium liquid phase composition can be calculated. It has to be mentioned that due to the GC measurements inaccuracy, an error is involved to the determination of the reservoir fluid and the gas phase (at each step) composition. So the estimation of liquid phase (at each step) composition may slightly deviate from the real one. This deviation is not significant for the case of high-concentration components in contrast it affects the low-concentration components and that's why the later were adjusted in case of concentration being slightly negative. Afterwards the whole composition was adjusted. This is the repeating procedure for the 5 steps of pressure of each sample. Experimental K-values at each pressure step can be calculated.

Experimental K-values are checked concerning their consistency at any pressure step using Standing's correlation that is a used for the calculation of K-values at any pressure step. The procedure and the equations that are used are the same to them that are used for the separator oil and gas K-values. The results will be presented to the next chapter.

BIBLIOGRAPHY

1. Gaganis, V., Kourlianski, E., Varotsis, N. (2017). An accurate method to generate composite PVT data for black oil simulation. Technical University of Crete.

5. RESULTS AND OBSERVATIONS.

The PVT-data-base has been separated and studied according to the PVT test that the samples have been submitted. The results of each study that has been implemented are presented at the following sub-chapters. These results are interpreted through diagrams that present the behavior of K-values for several samples at various pressure steps and temperatures.

5.1 K-VALUES OBTAINED FROM SINGLE STAGE FLASH LIBERATION OF BHS.

As mentioned in Chapter 4 the K-values of 265 bottom-hole samples are examined. The experimental K-values are compared with the K-values that arose from the Wilson correlation. Wilson correlation have been chosen to be implemented due to the simplicity of the method and because the conditions of the flash liberation are the atmospheric. Liquid and gas compositions are included to the PVT data-base. The range of the molar mass of the reservoir fluids that have been submitted to single stage flash liberation is presented to the diagram that follows (Figure 11).

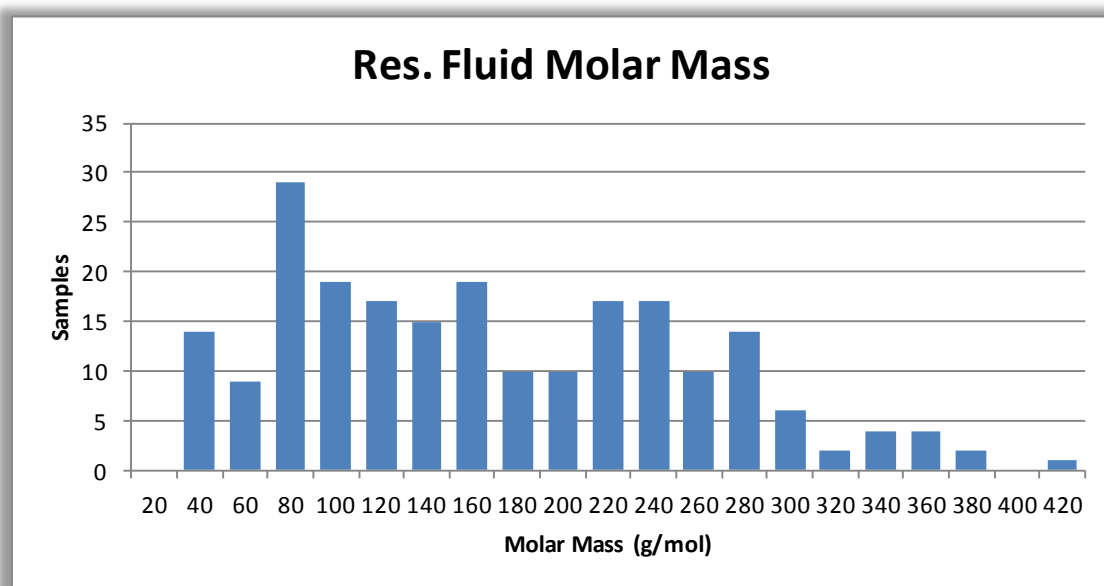


Figure 11: Frequency diagram of molar masses of BHS.

It is obvious that the molar mass of the reservoir samples extends over a wide range. Wilson K-values at atmospheric conditions are presented in Figure 12.

| K-C1 | K-C2 | K-C3 | K-C4 | K-C5 | K-C6 | K-C7 | K-C8 |
|--------|-------|------|------|------|------|------|------|
| 271,73 | 30,87 | 6,46 | 1,53 | 0,41 | 0,15 | 0,05 | 0,02 |

Figure 12: Wilson K-values at atmospheric conditions.

The comparison of Wilson and experimental K-values will take place at the diagram that follows (Figure 13).

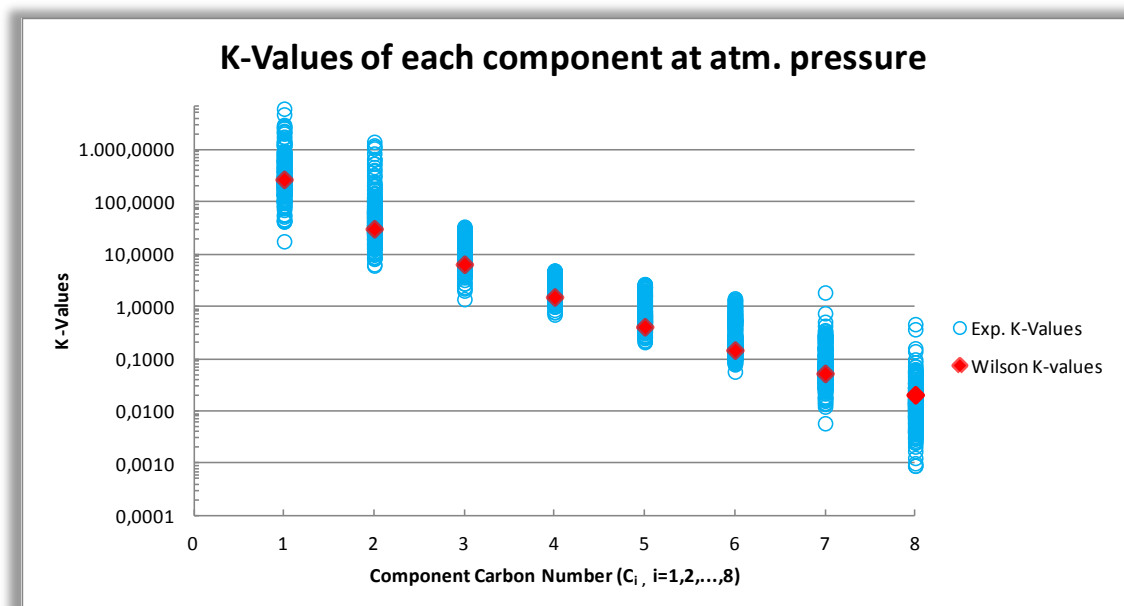


Figure 13: K-values of BHS at atmospheric pressure and temperature.

Only the K-values of the components up to C8 are examined because the experimental K-values of heavier components are not defined for the majority of the samples. It is obvious that the experimental K-values of the intermediate components (C3-C6) are in better agreement with the K-values that are defined from Wilson correlation. As the compounds get heavier or lighter the experimental K-values are getting a wide range. This is happening because for the light components like C1 the amount of the liquid phase is almost non-existent and this makes the experimental measurement very difficult and error-sensitive. On the other hand for the heavy components, like C8 the amount of gas phase is imperceptible and the K-value may be inaccurate.

5.2 K-VALUES OBTAINED FROM STOCK TANK OIL AND GAS OF RECOMBINED RESERVOIR SAMPLES.

The K-values of 291 recombined reservoir samples that obtain from a single stage flash at atmospheric conditions are examined at this study. Gas and liquid phase compositions that are used, are included to the PVT data base. The experimental K-values are compared with the Wilson K-values and this correlation has been chosen because is a simple, straight-forward correlation and the conditions are the atmospheric. The range of the molar masses of the RSS samples is presented to the Figure 14.

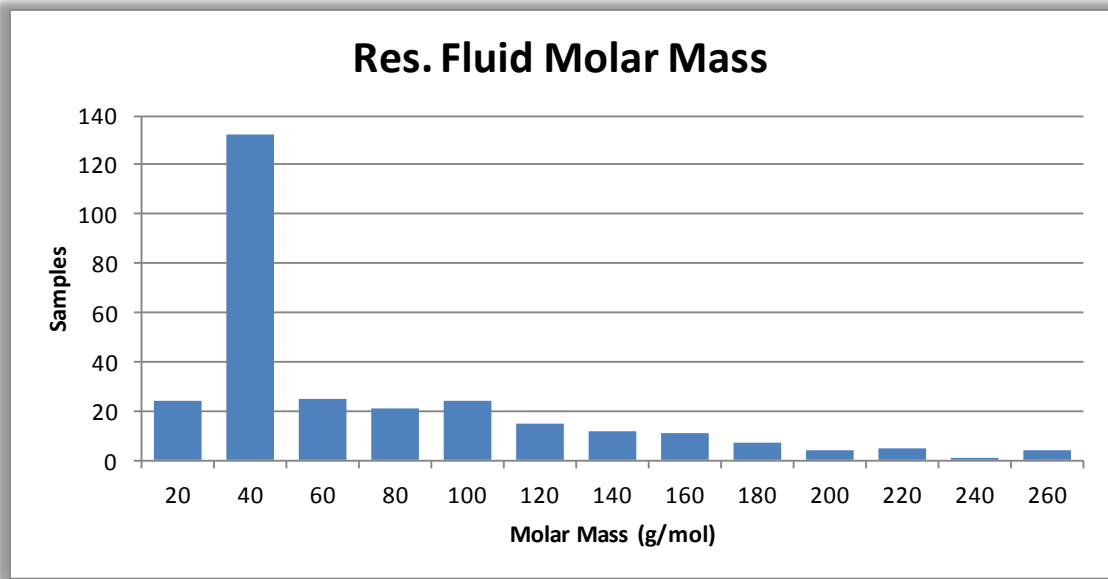


Figure 14: Frequency diagram of molar masses of RSS.

As it is shown to the diagram the majority of the samples are light fluids (gases) and the comparison to Wilson K-values is done with the next diagram (Figure 15).

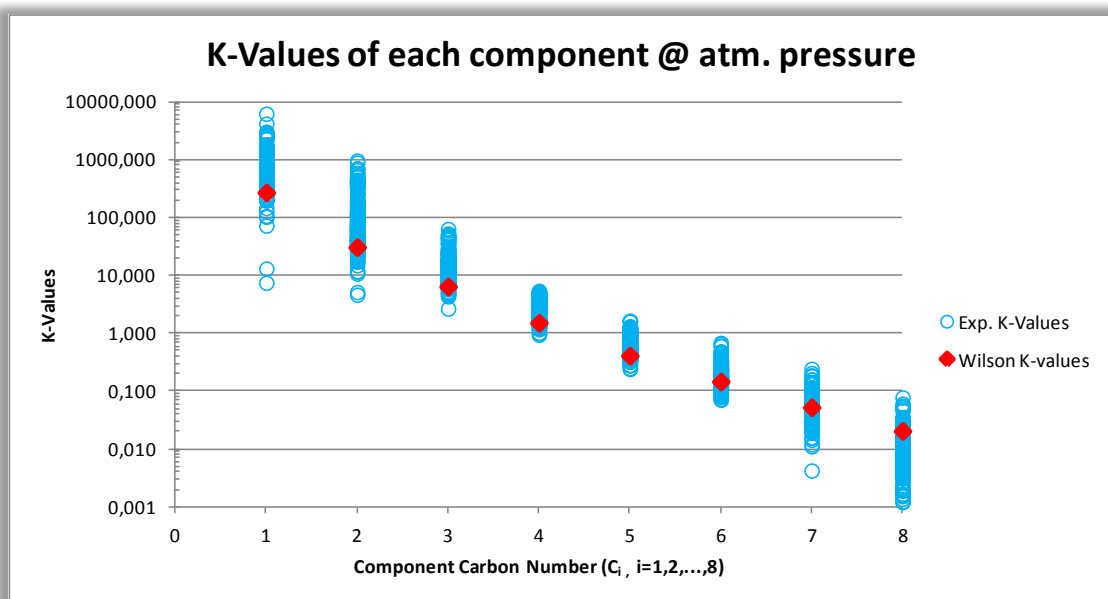


Figure 15: K-values of RSS at atmospheric pressure and temperature.

As it is expected the BHS and RSS experimental K-values at atmospheric conditions differentiate the same way to the K-values that have been calculated with the Wilson correlation.

5.3 K-VALUES OBTAINED FROM SEPARATOR OIL AND GAS OF RECOMBINED SAMPLES.

The recombined reservoir samples that have been examined as concerns their K-values at atmospheric conditions (sub-chapter 5.2) are now re-examined as concerns their K-values at separator conditions. The compositions of separator gas and liquid, which are used for the experimental K-values extraction, are included in the PVT data-base. The separator conditions are described by the next diagrams (Figure 16, Figure 17).

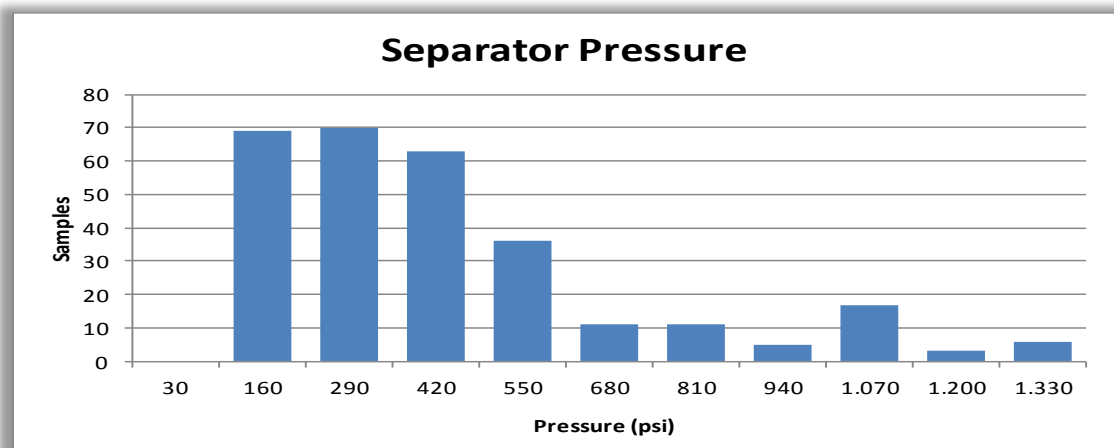


Figure 16: Frequency diagram of separator pressures.

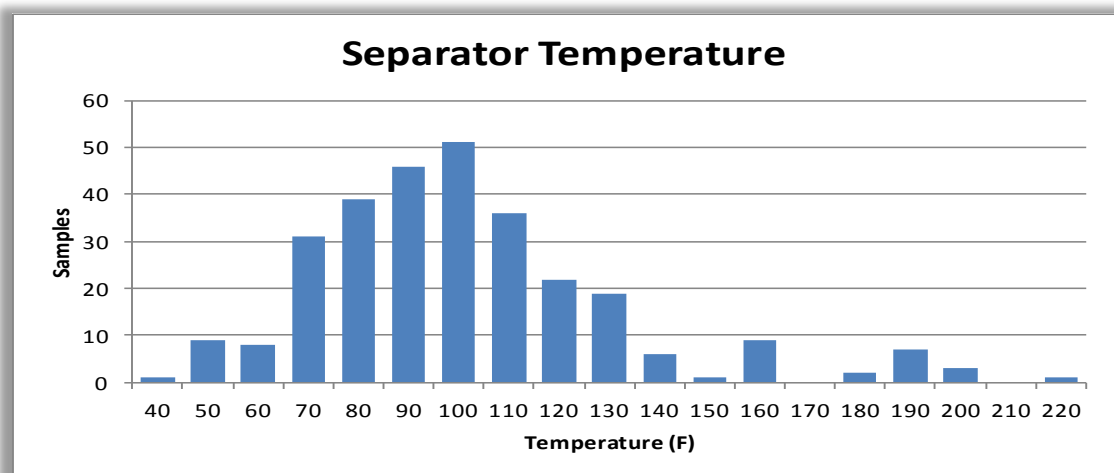


Figure 17: Frequency diagram of separator temperatures.

As anyone can observe to the upper diagrams there is a wide range of separator pressures and temperatures. The correlations that have been used for the extraction of K-values of each sample are the Standing's and Wilson. These two methods can be applied because the majority of the samples are flashed at pressures and temperatures below 1000 psi and 200 °F respectively. The K-values of each component will be examined separately starting from CH₄.

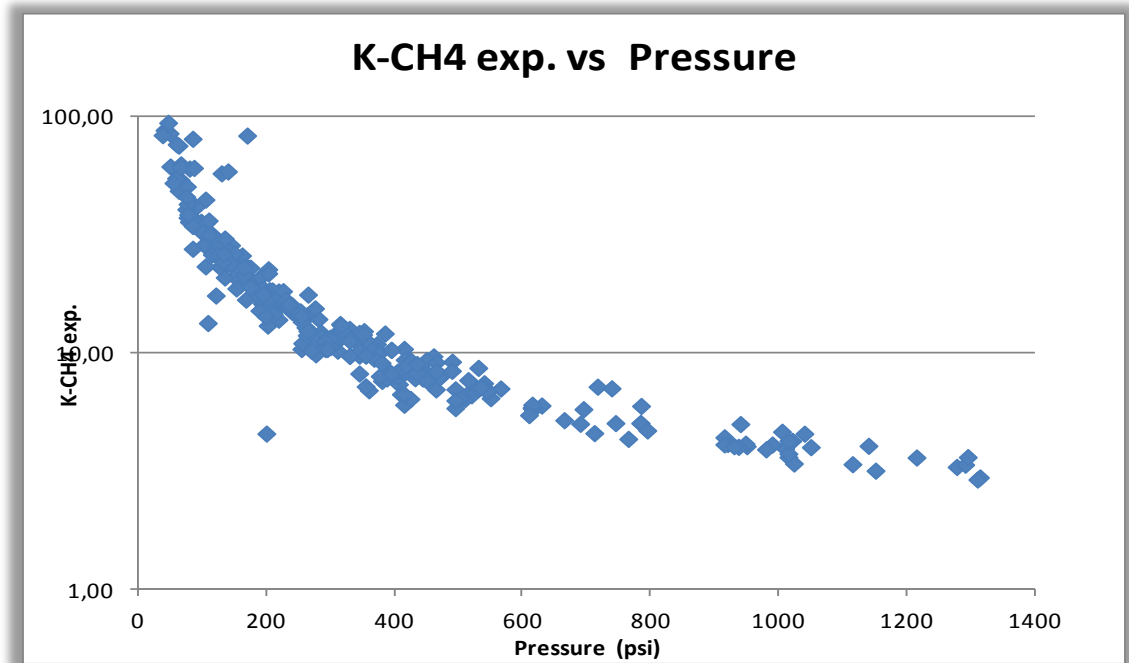


Figure 18: Experimental K-values of CH₄ vs. Pressure.

The experimental K-values of CH₄ have been plotted versus pressure. The behavior of the CH₄ K-values as the pressure increases is the expected one. Lower K-values arise as the pressure increases and higher as the pressure is approaching the atmospheric one. It has to be mentioned that the deviation of the K-values at the same pressure is caused by different temperatures. At a certain pressure as the temperature get increased higher K-values arise. It is obvious that at low pressures there are several values that deviate a lot from the typical shape (pressures around 200 psi). This high deviation cannot be attributed to different temperatures and this has been verified by checking the conditions of the flash of each outlier. The conclusion is that the K-values that not converge at all to the general shape are not reliable. It seems reasonable because the experimental measurement at such low pressures which result in low concentrations of liquid phase of CH₄ is very sensitive to errors. These outliers are not excluded from this study because the incorrect measurements may affect a lot the estimation of CH₄ K-value but they are considered inconsiderable to the total concentration estimation.

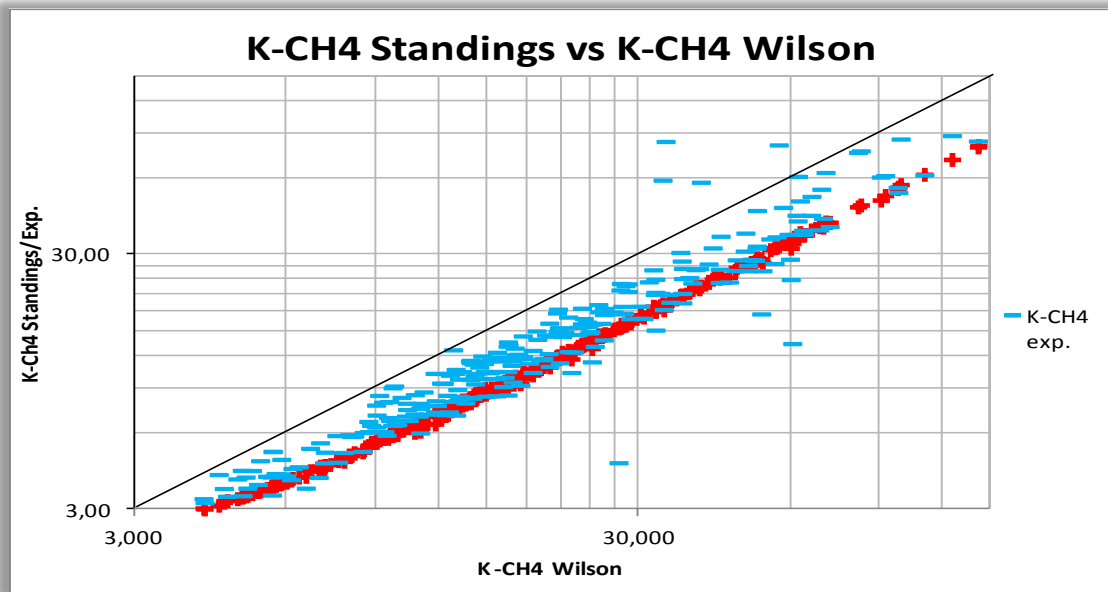


Figure 19: CH₄ Standing's K-values vs. CH₄ Wilson K-values.

The K-values of CH₄ that has been estimated with Standing's and Wilson correlation are compared to the upper diagram (Figure 19). Experimental K-values have been introduced also. The first observation is that there is a consistently disagreement between the two correlations results. Experimental K-values seem to be closer to the Standing's one. This consistently disagreement is happening because Wilson correlation produce higher K-values for CH₄ but this consistently disagreement is not a problem to the total composition estimation.

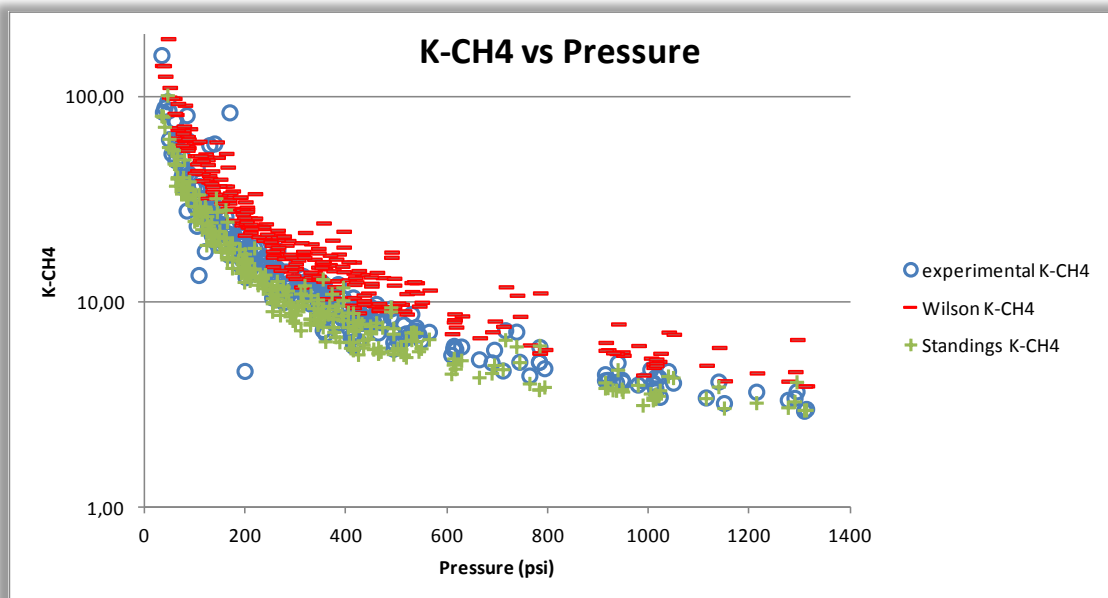


Figure 20: K-Values of CH₄ vs. Pressure.

Wilson, Standing's and experimental K-values have been plotted vs. pressure. The conclusion that is exported from the diagram is that the disagreement of the results is getting more intense as the pressure increases and that make sense because Wilson

and Standing's correlations are structured for low pressures K-values estimation. The behavior of these methods at higher pressures will be examined at next cases.

The experimental K-values of C_2H_6 have been plotted vs. pressure and are presented to the Figure 21.

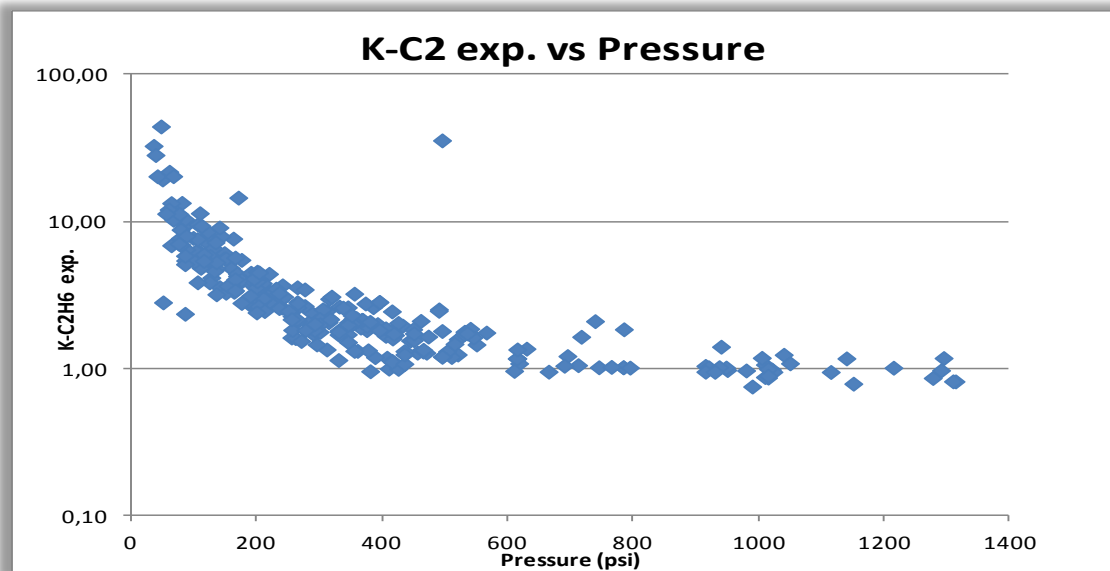


Figure 21: Experimental K-values of C_2H_6 vs. Pressure.

As it was expected the behavior of these K-values is similar to the behavior of CH_4 K-values. Small deviations are observed due to different temperatures and for one more time there are outliers due to experimental errors. It has to be mentioned that outliers of C_2H_6 are different to the CH_4 outliers.

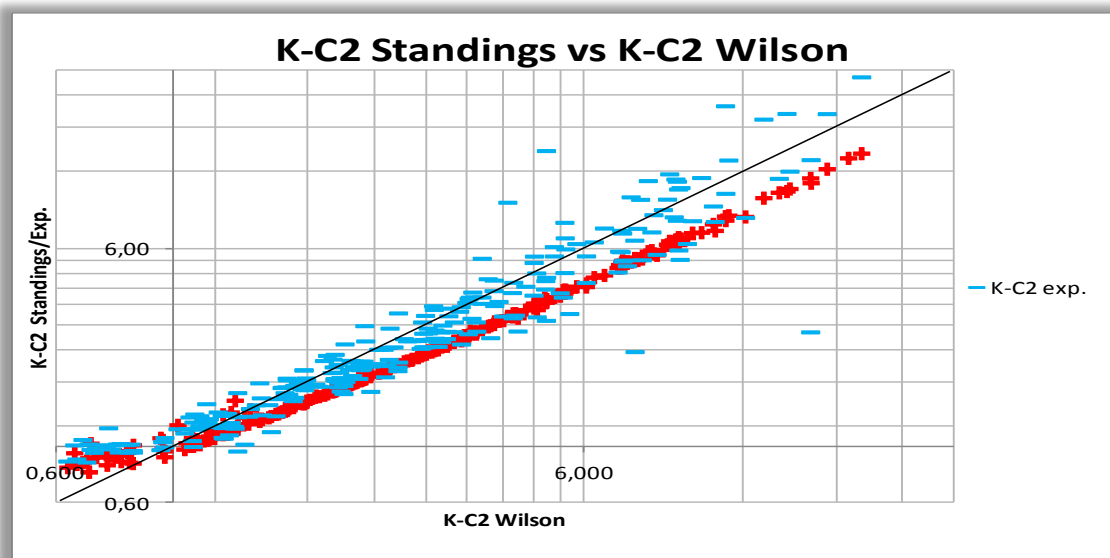


Figure 22: C_2H_6 Standing's K-values vs. C_2H_6 Wilson K-values.

The K-values of C_2H_6 that has been estimated with Standing's and Wilson correlation are compared to the upper diagram (Figure 22). Experimental K-values have been

introduced also. At high pressures (low K-values) there is a better agreement between the experimental K-values and the K-values estimated by the two methods. This is happening because the liquid phase C_2H_6 concentration gets increased so the experimental measurements being more accurate and the sensitivity to error of the correlations get decreased.

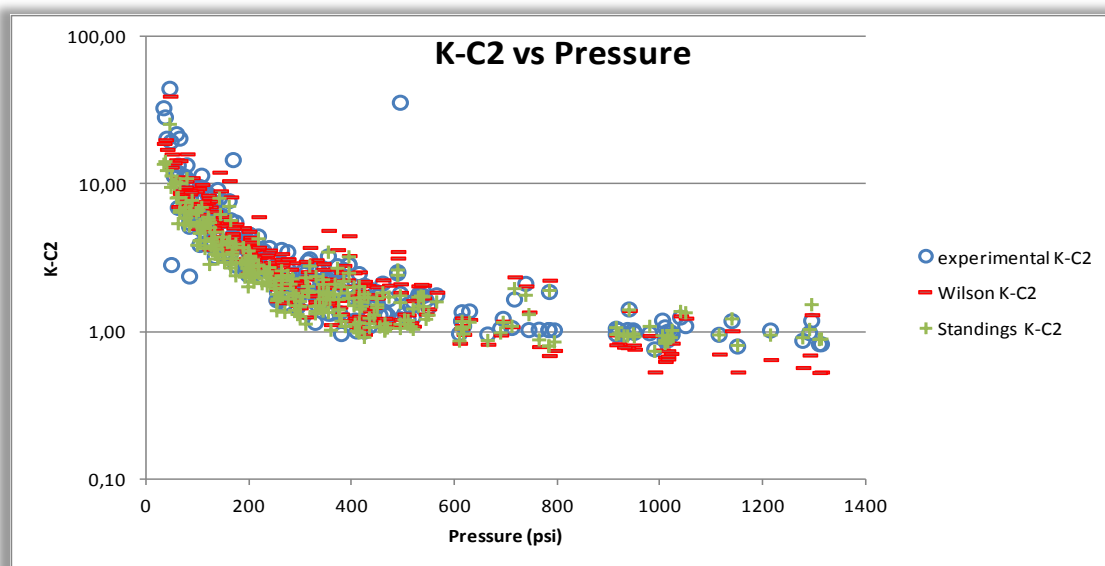


Figure 23: K-Values of C_2H_6 vs. Pressure.

Experimental, Wilson and Standing's K-values have been plotted versus several pressures. A good matching is observed between the three types of K-values at the whole range of pressures. The samples that have been flashed at higher pressure are fewer and their K-values observation can be more detailed. Standing's K-values seem to agree more with the experimental and Wilson K-values seem to deviate from the other two.

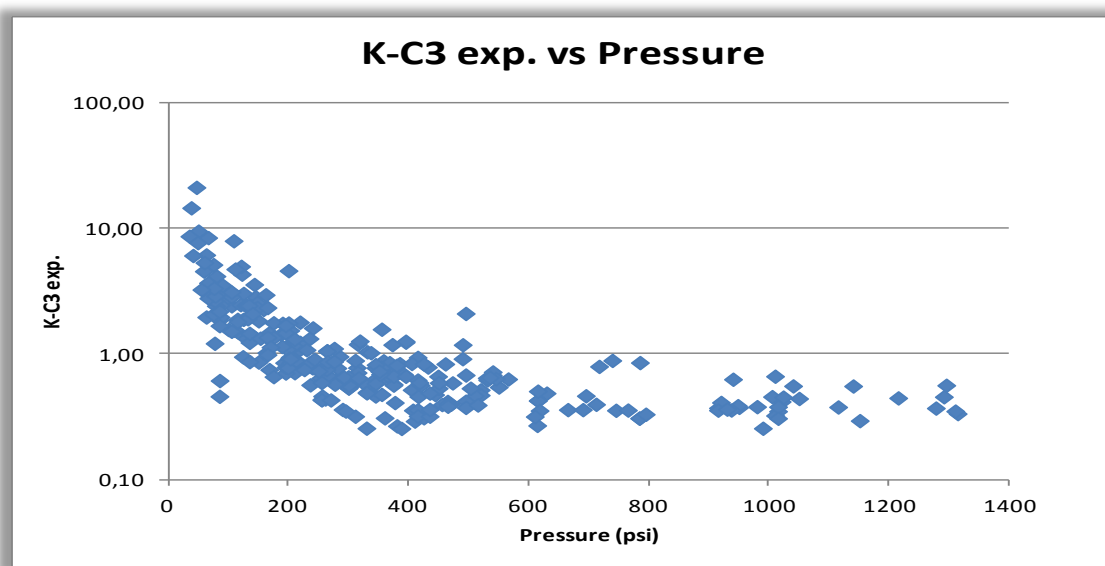


Figure 24: Experimental K-values of C_3H_8 vs. Pressure.

Experimental K-values of C_3H_8 have been plotted versus Pressure. The behavior of the K-values is similar to the previous plots of CH_4 and C_2H_6 but fewer outliers are observed. The explanation is that as the compounds get heavier the compositions of gas and liquid phase can be compared as concern their magnitude. In other words both of the two phases exist in considerable amounts and the experimental measurements are not such sensitive to errors.

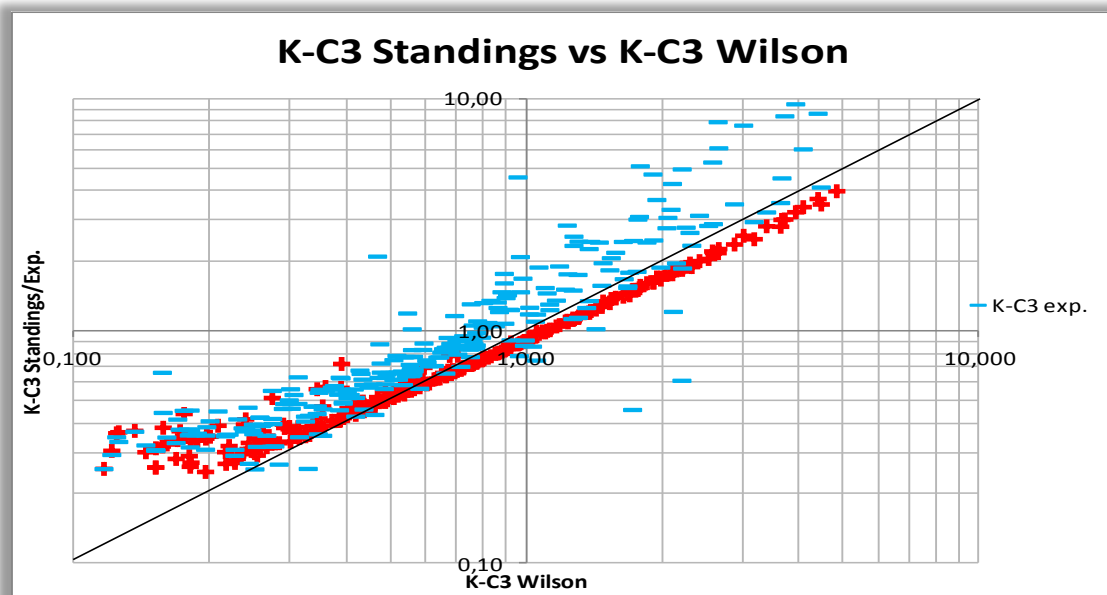


Figure 25: Standing's C_3H_8 K-values vs. Wilson K-values.

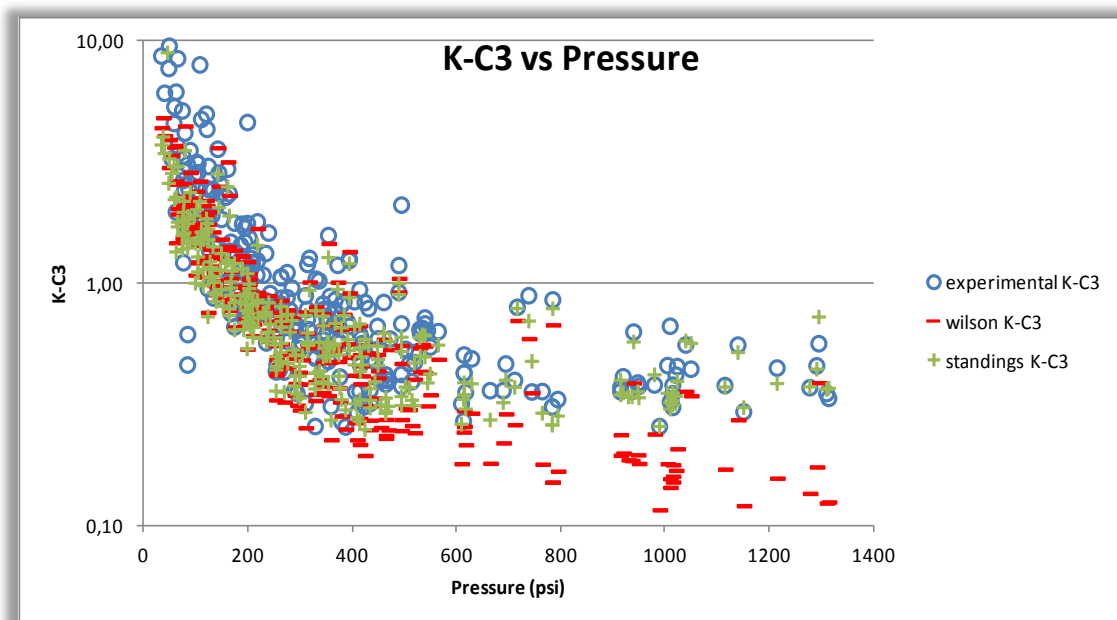


Figure 26: K-Values of C_3H_8 vs. Pressure.

By the comparison of Standing's with Wilson K-values at Figure 25, a satisfied agreement between them is observed and is more intense at low pressures. On the other hand the experimental K-values seem to be consistently higher with greater

deviation at low pressures. This deviation is un-considerable as the scale is small. C_3H_8 is a light component and the low liquid concentration (high-sensitivity to errors of experimental measurement) at low pressures explains the deviation which has been preloaded. By plotting the ensemble of the estimated K-values versus pressure (Figure 26) a total agreement is observed. More specifically at low pressures Wilson K-values seem to be in accordance with the Standing's K-values and at higher pressures the later seem to follow the experimental more than the Wilson K-values.

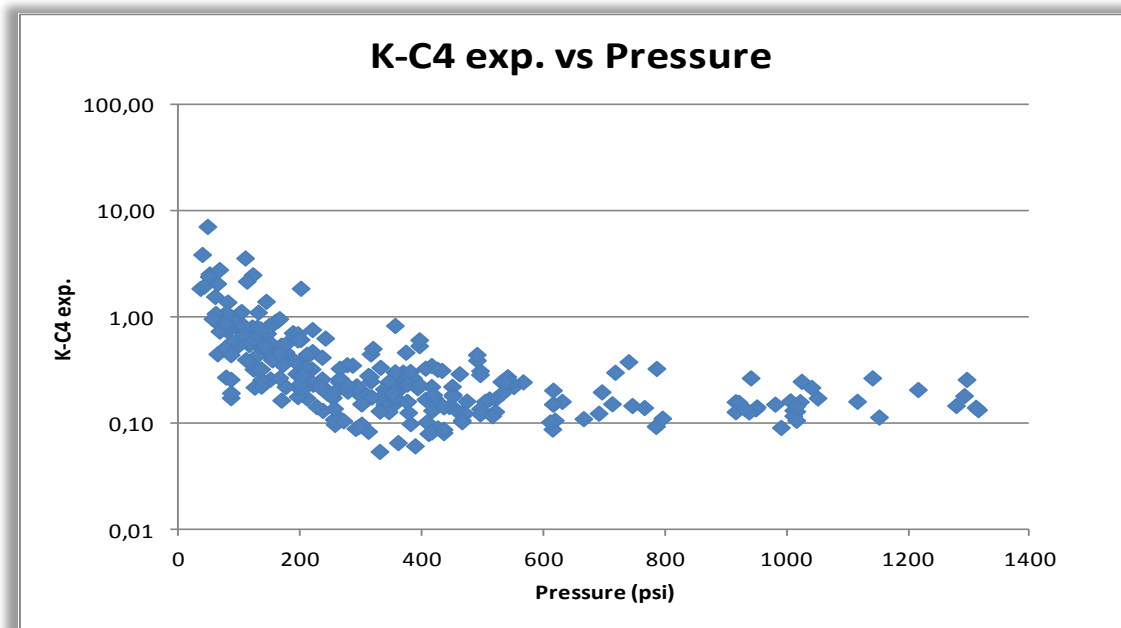


Figure 27: Experimental K-values of C_4H_{10} vs. Pressure.

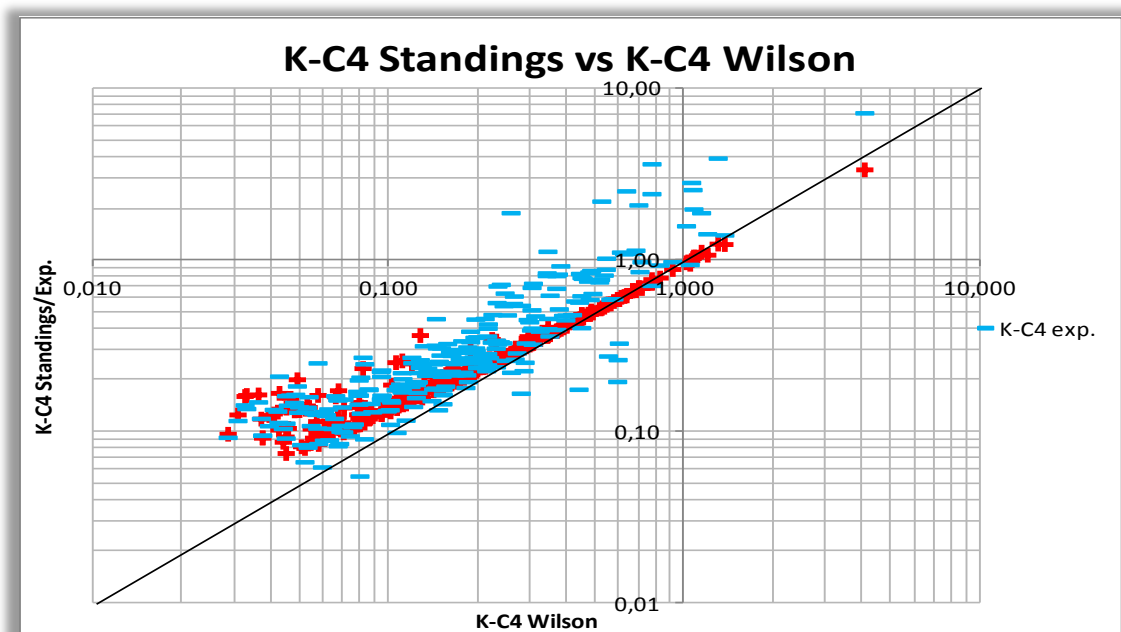


Figure 28: C_4H_{10} Standing's K-values vs. C_4H_{10} Wilson K-values.

The diagram of C_4H_{10} experimental K-values versus pressure and the comparison diagram of experimental, Standing's and Wilson K-values are displayed above. As shown to the Figure 27 as the components get heavier, less outliers are getting identified. In Figure 28 a total agreement between different method K-values is observed. It has to be mentioned that the scale is very small.

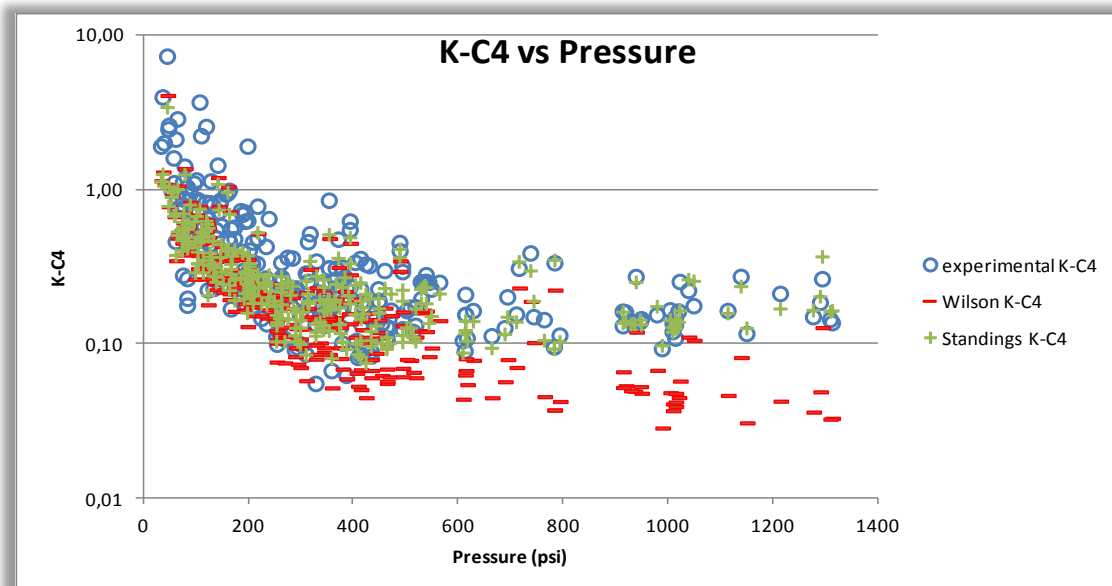


Figure 29: K-Values of C_4H_{10} vs. Pressure.

The ensemble of the estimated K-values has been plotted versus pressure at the diagram above (Figure 29). At low pressures Wilson are in accordance with Standing's K-values and on the other hand at higher pressures Standing's K-values comply with the experimental.

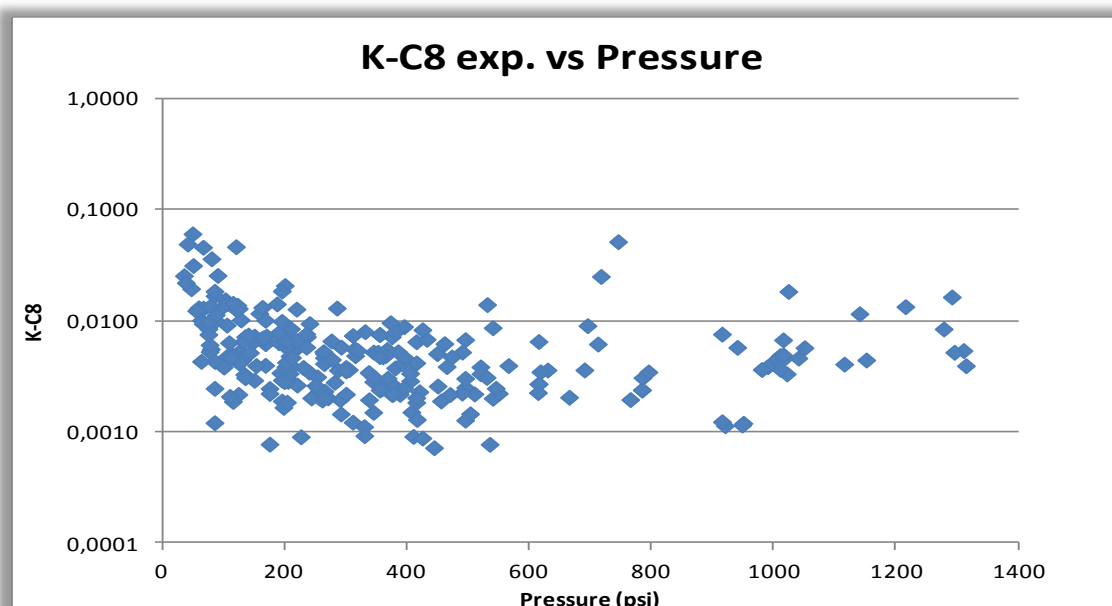


Figure 30: Experimental K-values of C_8H_{18} vs. Pressure.

The last component whose the K-values have been plotted versus pressure is the C_8H_{18} . This component have been chosen because is the heaviest one that a satisfactory number of experimental K-values is defined. The shape that describes the behavior of C_8H_{18} is similar to the typical one. That means that as the pressure increases a small part of the curve with decreasing trend is observed and after reaching the minimum, the curve is characterized by an increasing trend and reaches to the unity at the convergence pressure. As the separator pressures are not high the increasing part of the curve is not extended but there are several samples that create that part of the curve and give K-values higher than the intermediate pressure K-values.

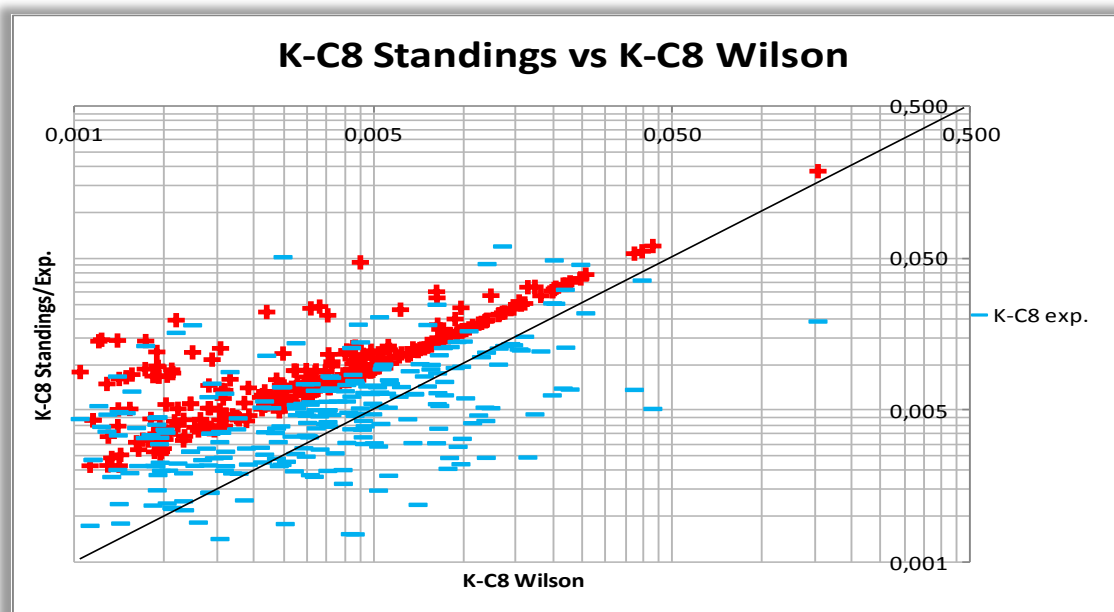


Figure 31: C_8H_{18} Standing's K-values vs. C_8H_{18} Wilson K-values.

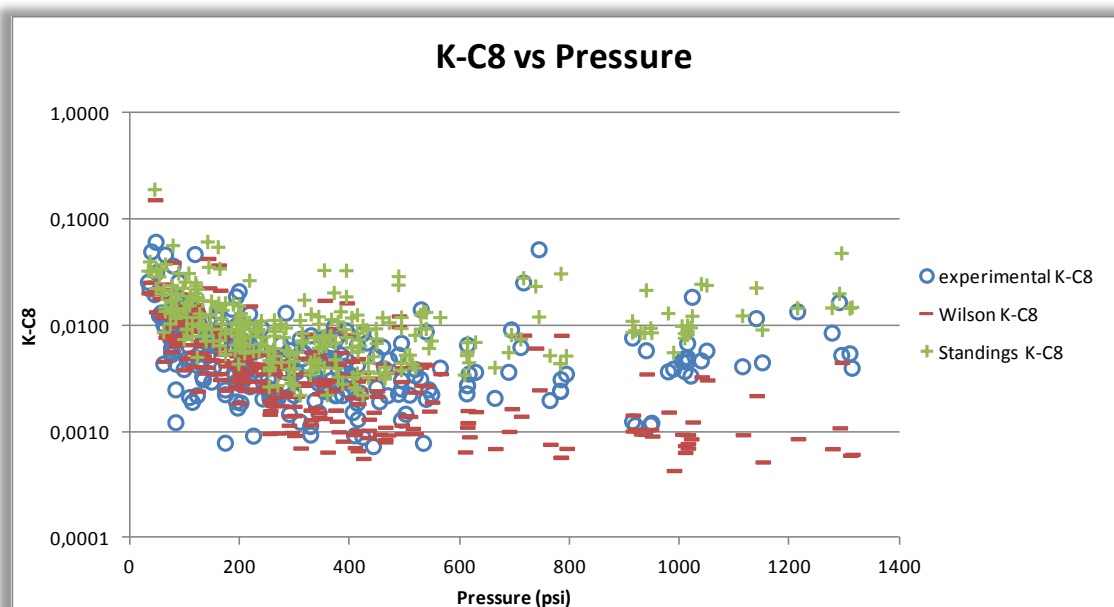


Figure 32: K-Values of C_8H_{18} vs. Pressure.

In the comparison diagram (Figure 31) an acceptable agreement is observed. As it is shown the scale is too small so the values are very close. The remarkable observations are 2. The first one is that as the compounds get heavier the experimental K-values are done less accurate because the gas phase composition is in-considerable but this is not a major obstacle to the total composition of equilibrium gas and liquid phase estimation and their properties determination. The second thing that has to be mentioned is that once more at low pressures Wilson are in accordance with Standing's K-values and on the other hand at higher pressures Standing's K-values comply with the experimental.

5.4 K-VALUES OBTAINED AT ANY PRESSURE STEPS OF DIFFERENTIAL LIBERATION EXPANSION.

At the following sub-chapter the K-values that obtain at each pressure step of DLE experiment are examined. 190 reservoir fluid samples, that are recombined or bottom-hole, are flashed at several pressure steps starting from the saturation pressure of each sample. The temperature, saturation pressure and molar mass range of the samples that were used are described by the following frequency diagrams.

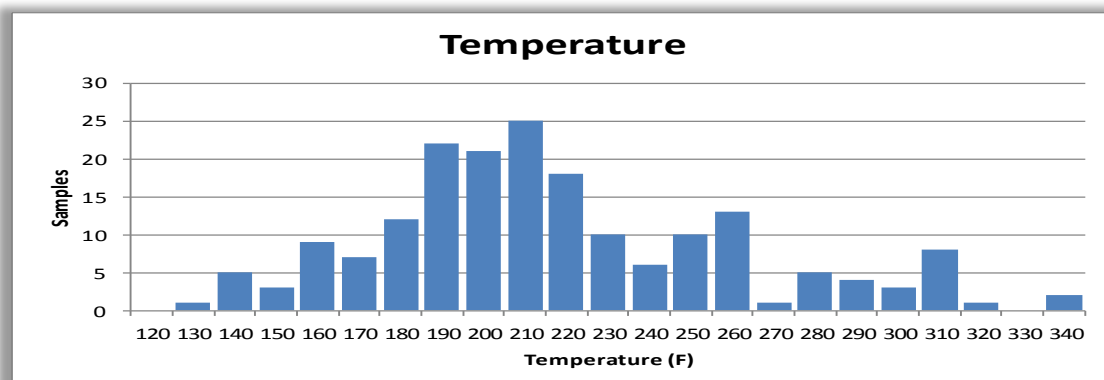


Figure 33: Frequency diagram of temperatures of Differential Liberation Expansion experiment.

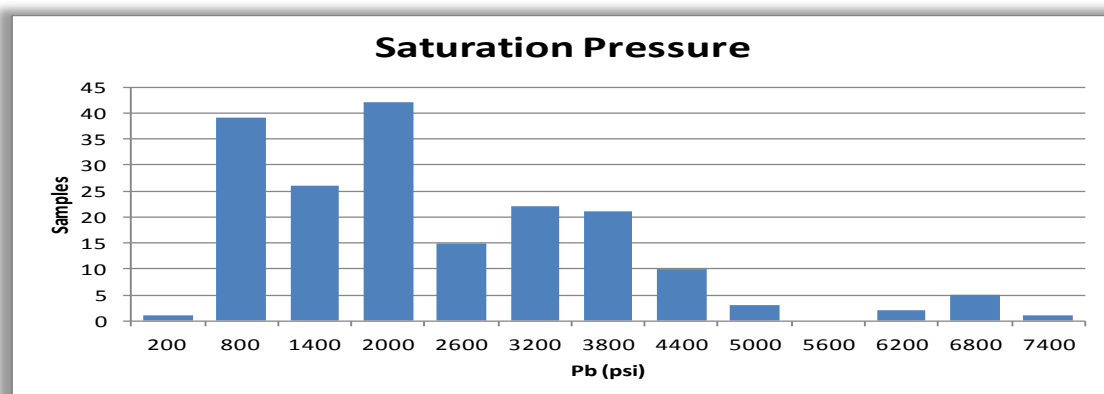


Figure 34 : Frequency diagram of reservoir fluid samples saturation pressure.

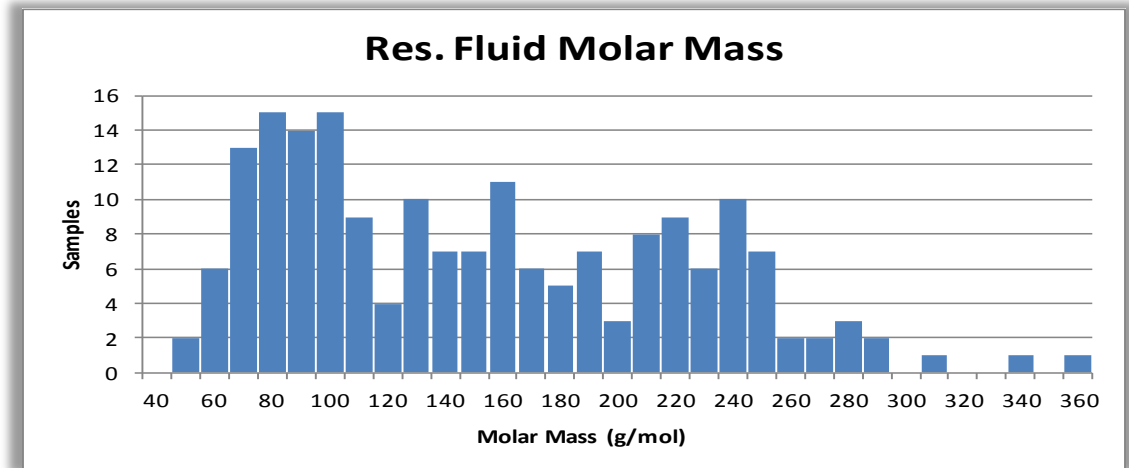


Figure 35: Frequency diagram of the reservoir fluid (DLE experiment submitted) molar masses.

The samples that have been submitted to the DLE experiment have been flashed at several pressure steps. The first 5 steps (with the first one to be right after the saturation pressure) have been chosen for the evaluation of the K-values that obtain at each case. The compositions of the reservoir fluids and the extracted gas phase composition at each pressure step are included in the PVT data base. For the calculation of the experimental K-values at each pressure step of the DLE the equilibrium liquid phase composition is needed and is calculated mathematically as mentioned in the sub-chapter 4. Samples whose components composition is slightly negative may be corrected and if the error is greater the sample is rejected. Standing's correlation has been selected for the estimation of K-values at each pressure step. The results are compared with the experimental K-values for each component starting from CH₄ at the first pressure step.

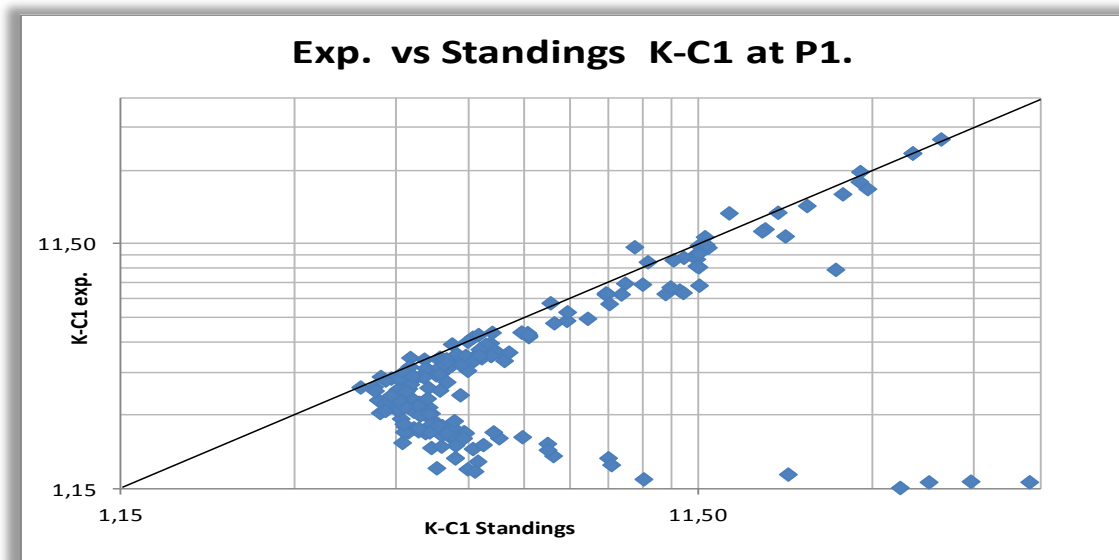


Figure 36: Experimental K-values of CH₄ versus Standing's K-values of CH₄ at P₁.

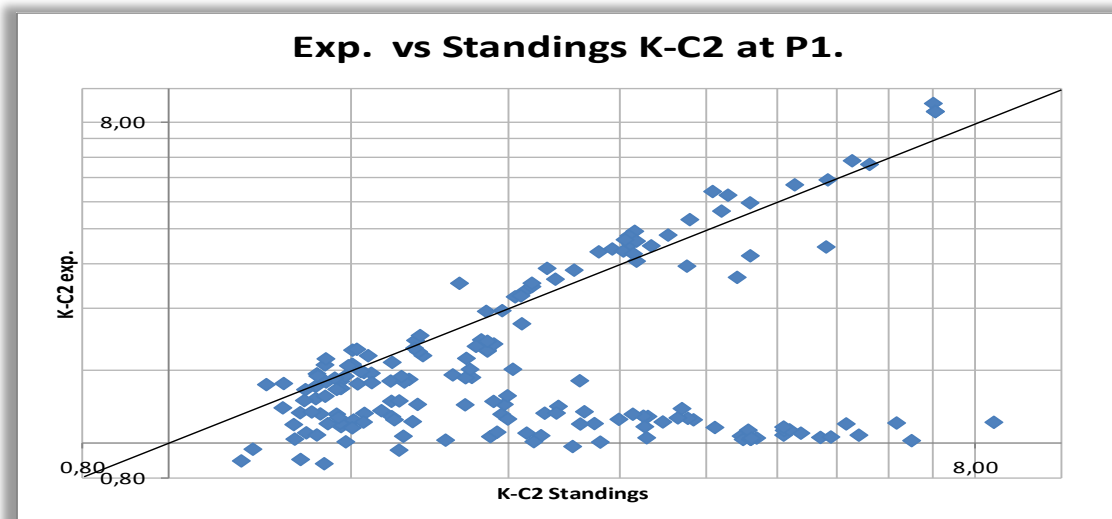


Figure 37: Experimental K-values of C₂H₆ versus Standing's K-values of C₂H₆ at P₁.

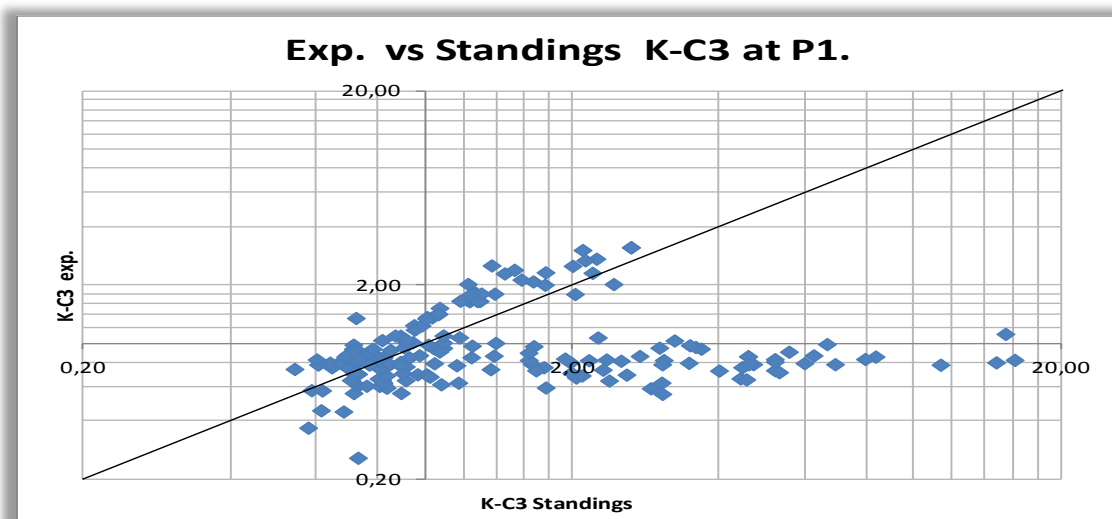


Figure 38: Experimental K-values of C₃H₈ versus Standing's K-values of C₃H₈ at P₁.

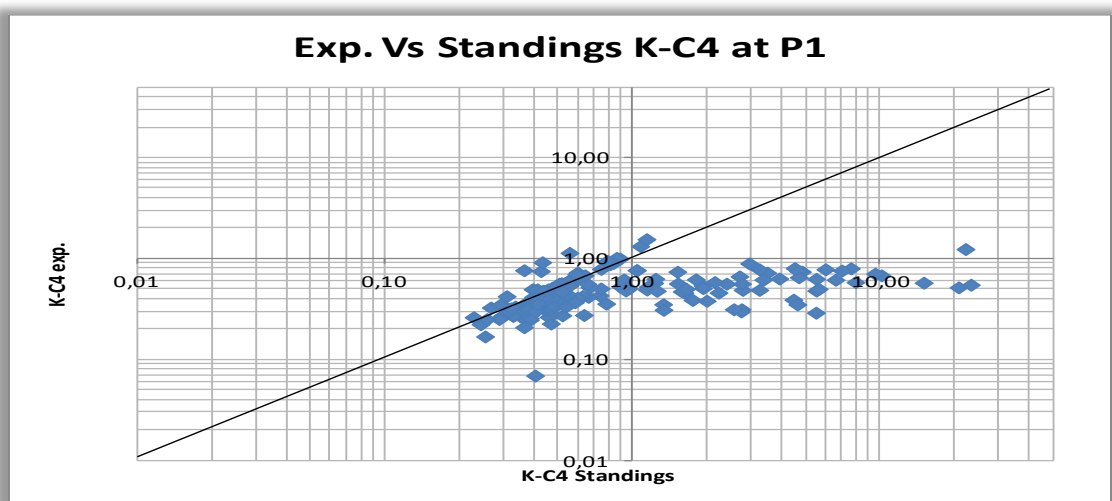


Figure 39: Experimental K-values of C₄H₁₀ versus Standing's K-values of C₄H₁₀ at P₁.

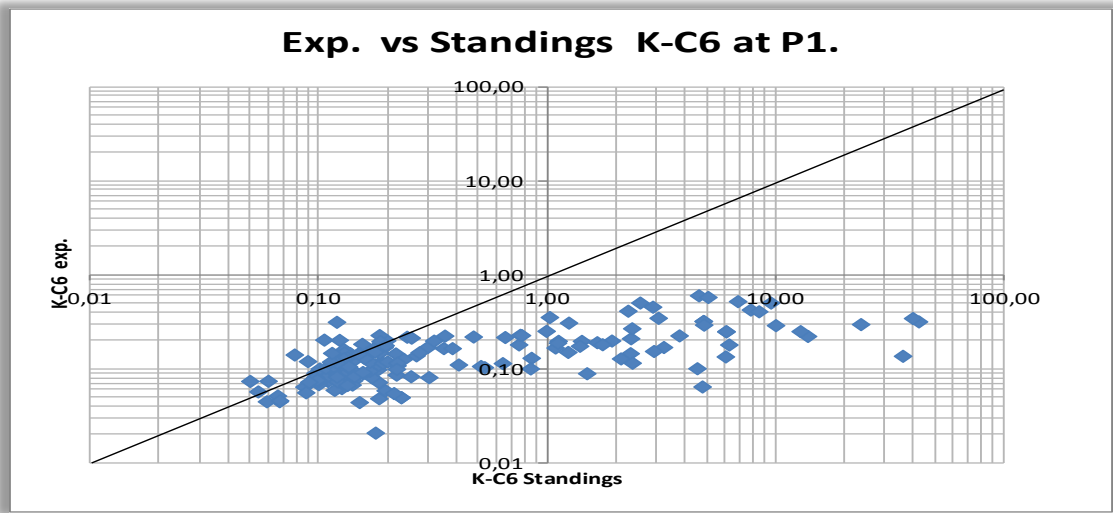


Figure 40: Experimental K-values of C_6H_{12} versus Standing's K-values of C_6H_{12} at P_1 .

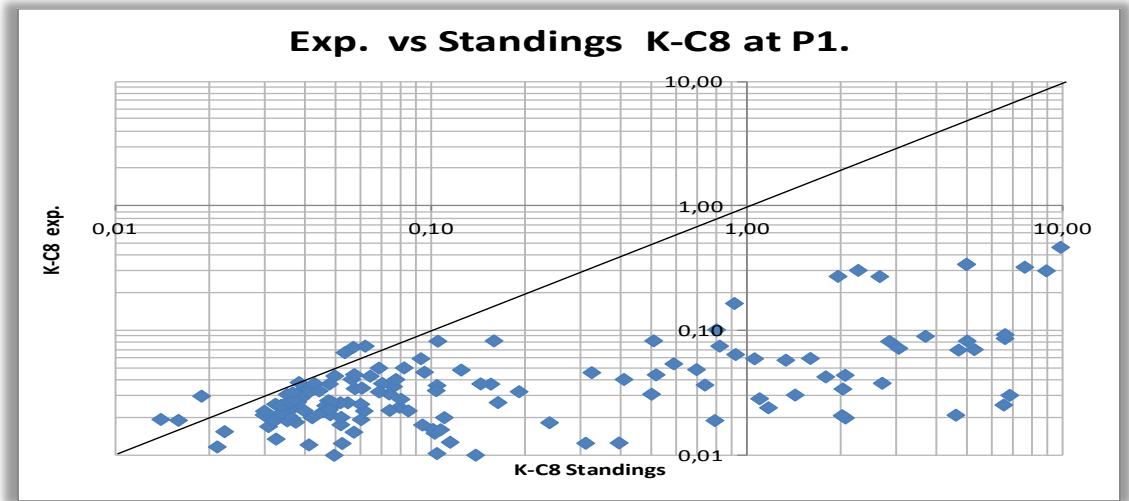


Figure 41: Experimental K-values of C_8H_{14} versus Standing's K-values of C_8H_{14} at P_1 .

As it is shown to the above figures the ratio of the reasonable values that indicate agreement to the outliers is almost the same for all the components and is almost 60/40 respectively. The first observation that is confirmed once more is based on the previous studies and concerns the errors of the experimental measurement of the composition of the heavy and light components. For example the C_8H_{14} equilibrium gas phase concentration is diminutive and combined with the slight concentration of the same component in the liquid phase makes the definition of the experimental K-values doubtful. In addition the mathematical calculation of the equilibrium liquid phase composition may also be inaccurate for the same reasons. The diagram in the Figure 42 shows the low concentrations in C_8H_{14} of the reservoir fluid but also of the equilibrium gas and liquid at the first pressure step. It is reasonable that as the pressure declines to the next pressure steps the gas phase concentration in C_8H_{14} will get increased and the opposite will happen for CH_4 .

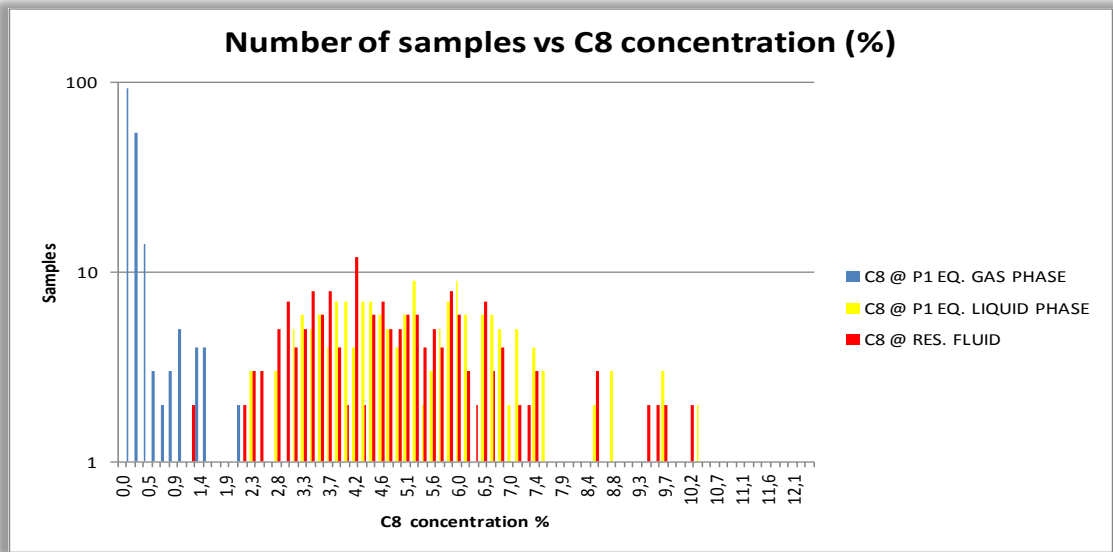


Figure 42: C_8H_{14} concentration of equilibrium gas and liquid phase at P_1 and reservoir fluid.

As mentioned before the ratio of the reasonable values that indicate agreement to the outliers is almost the same for all the components and is almost 60/40 respectively. Intermediate components deviation between Standing's and experimental K-values cannot be attributed to Errors in experimental measurements of composition and mathematical estimation of liquid phase composition. The other fact that is observed and strengthens the deviation between correlation and experimental K-values is that an interpolation is observed in Standing's correlation up to 2000 psi and after that follows an extrapolation at higher pressures.

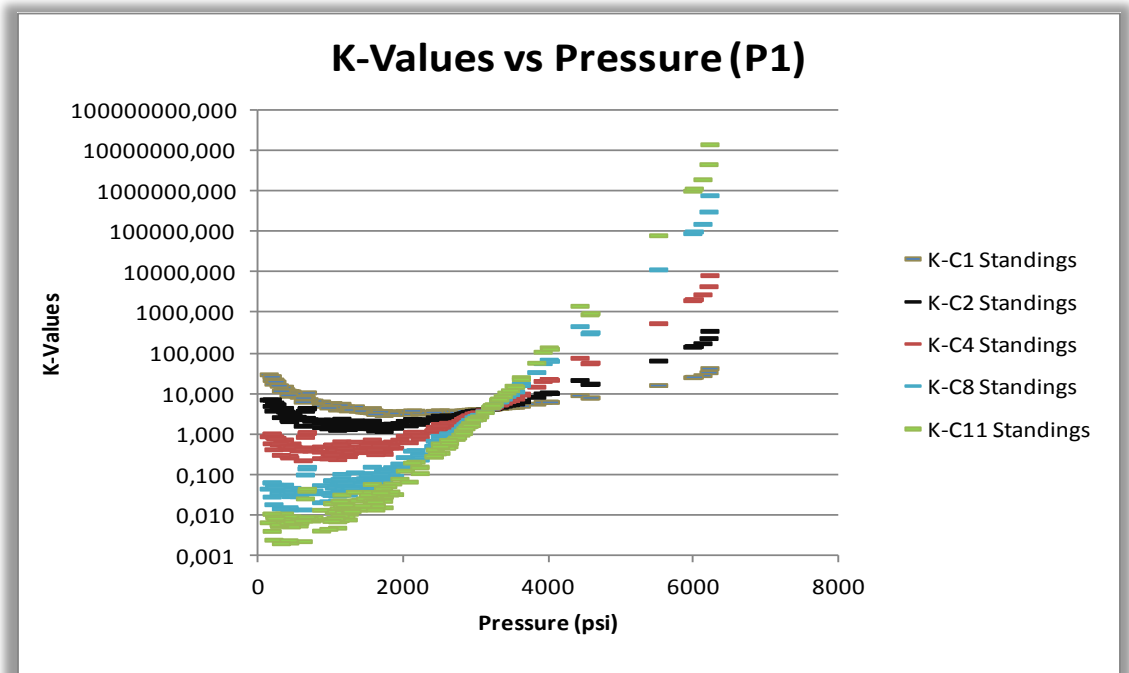


Figure 43: Standing's K-values versus Pressure at P_1 .

It is obvious that the behavior of Standings K-values as the pressure increases is not physically sound. As shown in the diagram above (Figure 43) as the pressure increases the K-values of all the components get increased also. That means that there is an increase of the volume as the pressure increases and this is not valid.

At next the comparison diagrams of experimental and Standing's K-values will be presented for the third pressure step of the DLE.

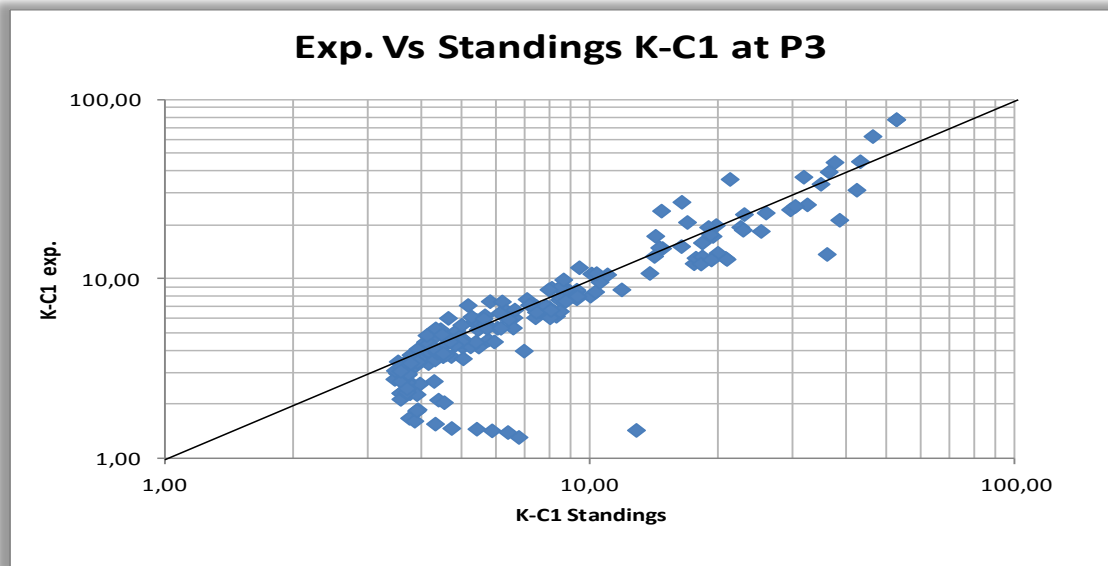


Figure 44: Experimental K-values of CH_4 versus Standing's K-values of CH_4 at P_3 .

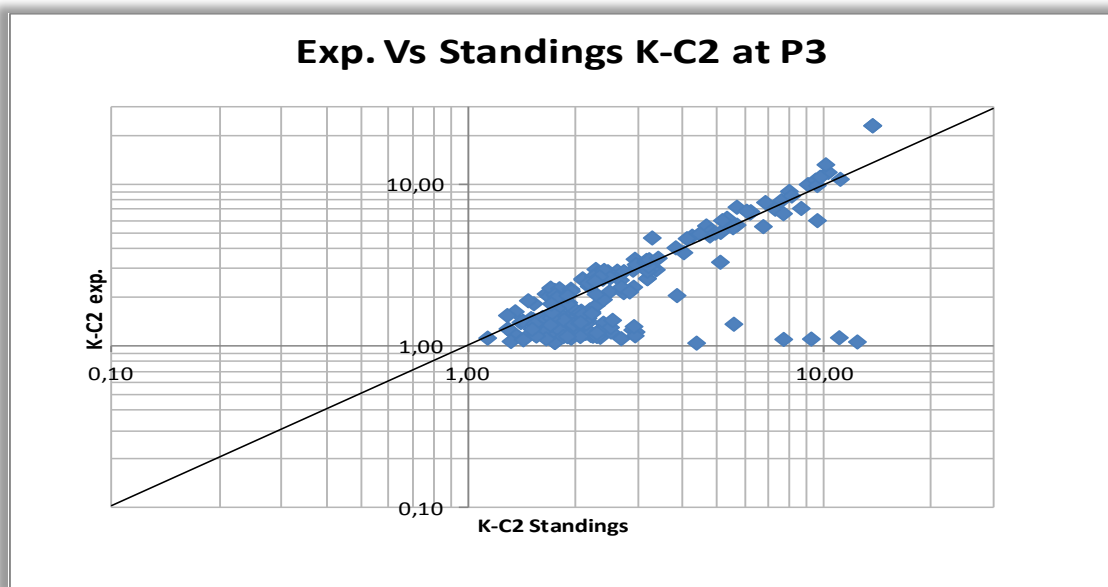


Figure 45: Experimental K-values of C_2H_6 versus Standing's K-values of C_2H_6 at P_3 .

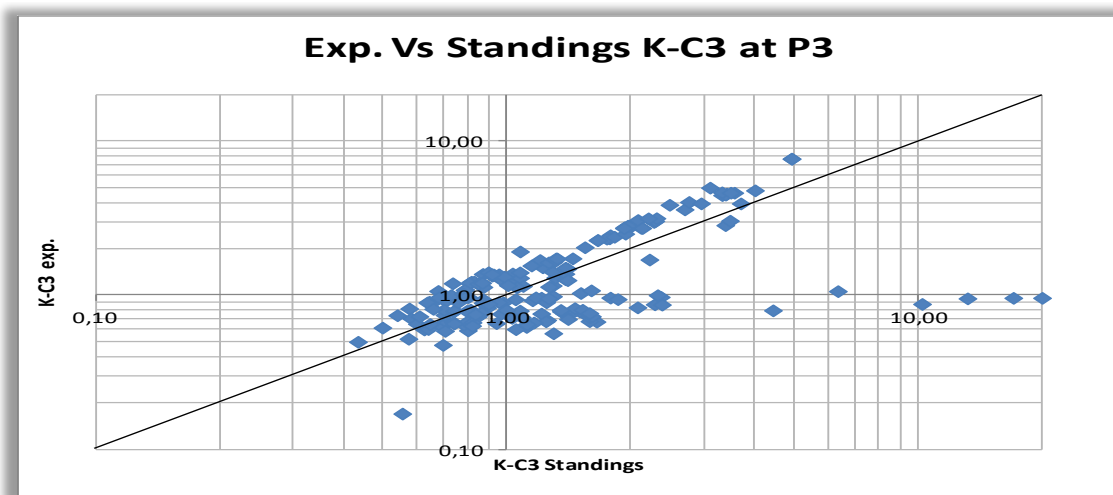


Figure 46: Experimental K-values of C_3H_8 versus Standing's K-values of C_3H_8 at P_3 .

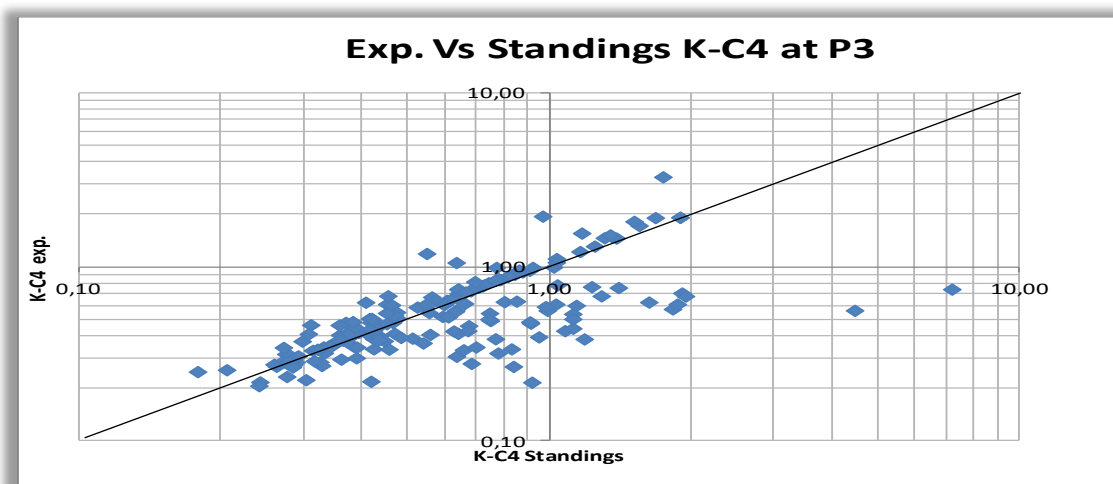


Figure 47: Experimental K-values of C_4H_{10} versus Standing's K-values of C_4H_{10} at P_3 .

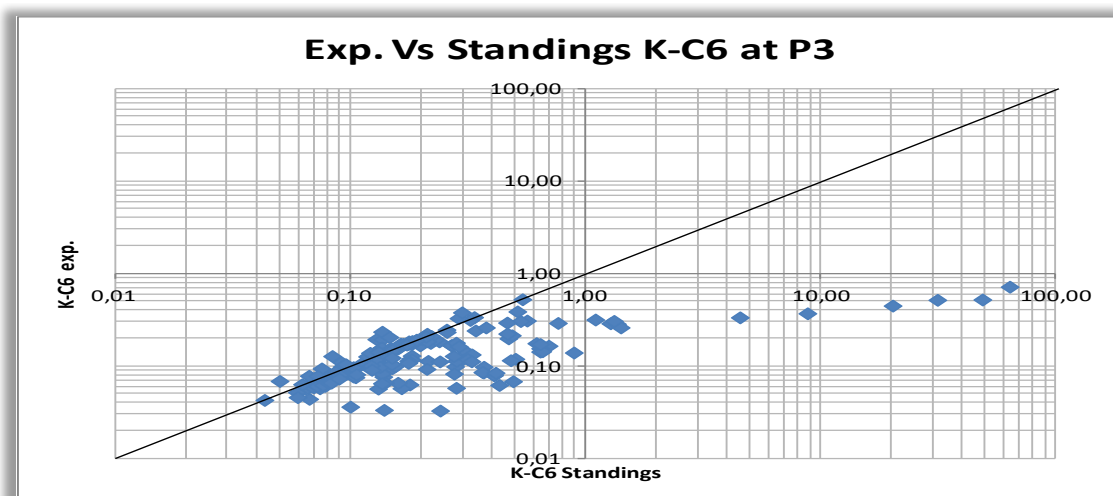


Figure 48: Experimental K-values of C_6H_{12} versus Standing's K-values of C_6H_{12} at P_3 .

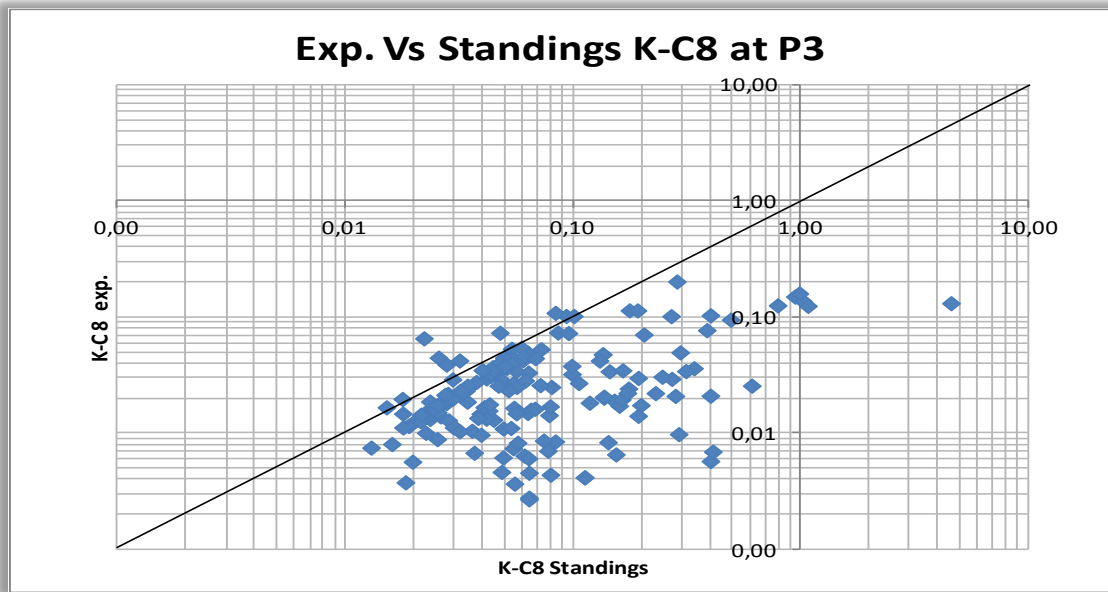


Figure 49: Experimental K-values of C_8H_{14} versus Standing's K-values of C_8H_{14} at P_3 .

A better matching between Standing's K-values and the experimental K-values is observed. That sounds reasonable because the pressures at the 3rd pressure step of the DLE are lower. The behavior of the Standing's correlation can be described by the next diagram (Figure 50). As it is shown the extrapolation of the correlation gets limited but there are high-pressure outliers for this step also. It has to be mentioned that as the DLE steps are going ahead the error of the mathematical determination of the equilibrium liquid phase composition getting bigger. Each DLE step error is added to the next one.

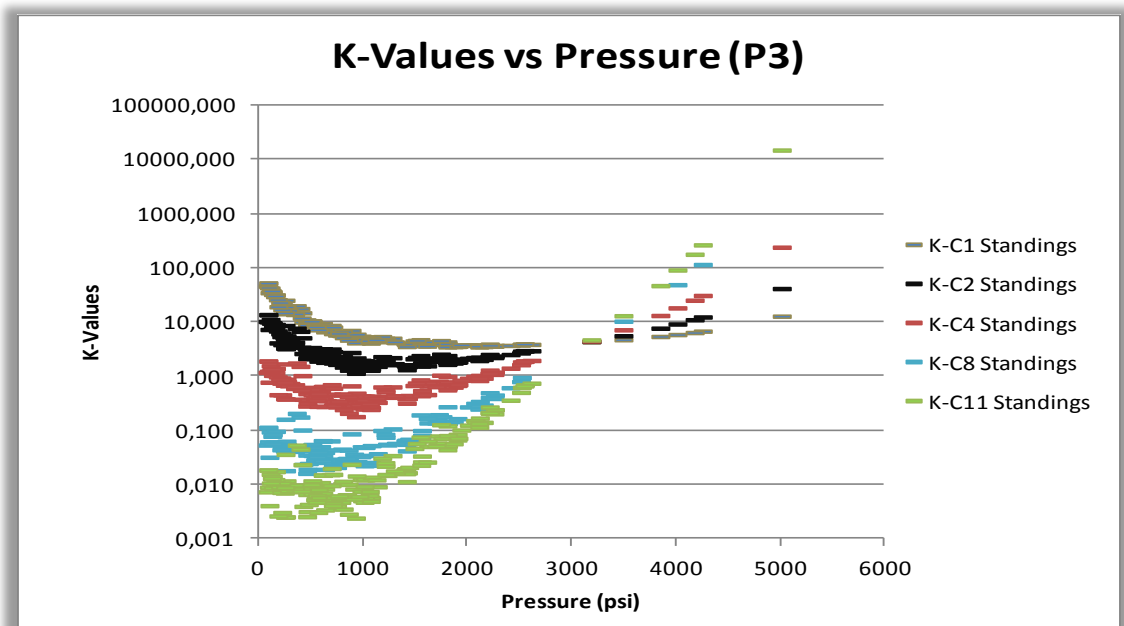


Figure 50: Standing's K-values versus Pressure at P_3 .

The comparison diagrams of experimental vs. Standing's K-values for the last pressure step are presented below. The best matching between the K-values is expected as the pressures are lower than the previous DLE steps. On the other hand the errors due to the mathematical estimation of the equilibrium liquid composition are getting their maximum magnitude.

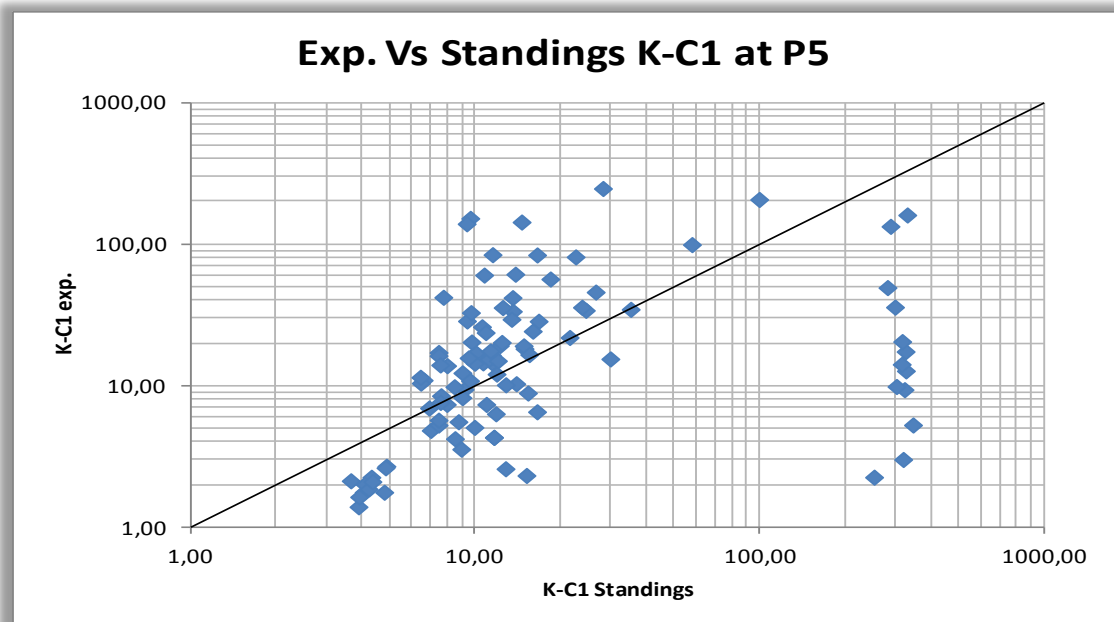


Figure 51: Experimental K-values of CH₄ versus Standing's K-values of CH₄ at P₅.

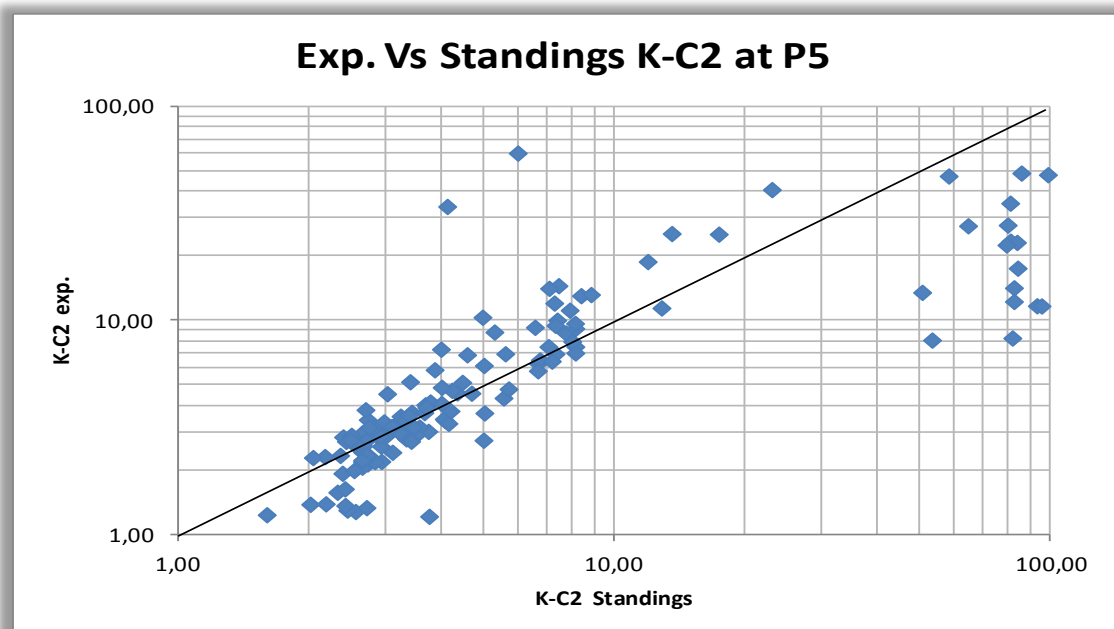


Figure 52: Experimental K-values of C₂H₆ versus Standing's K-values of C₂H₆ at P₅.

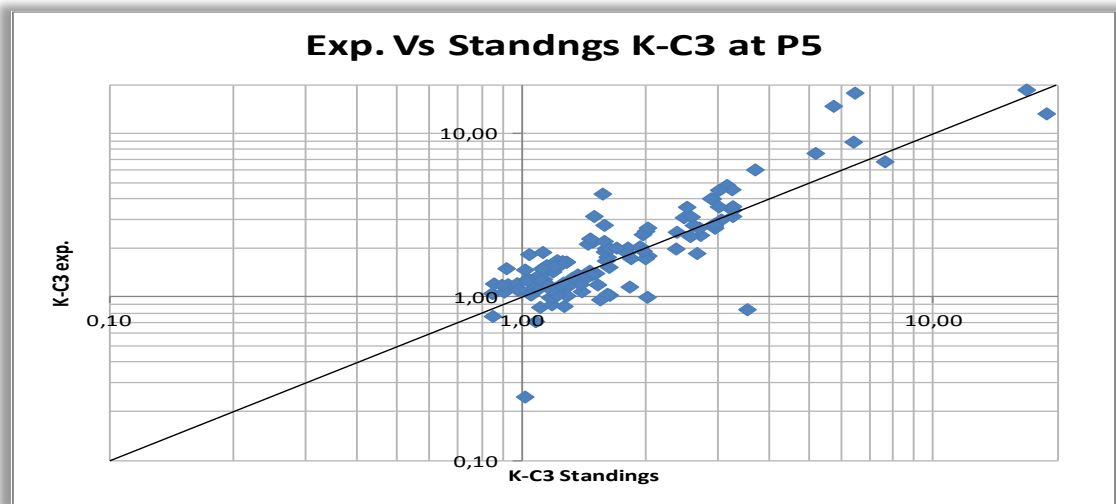


Figure 53: Experimental K-values of C_3H_8 versus Standing's K-values of C_3H_8 at P5.

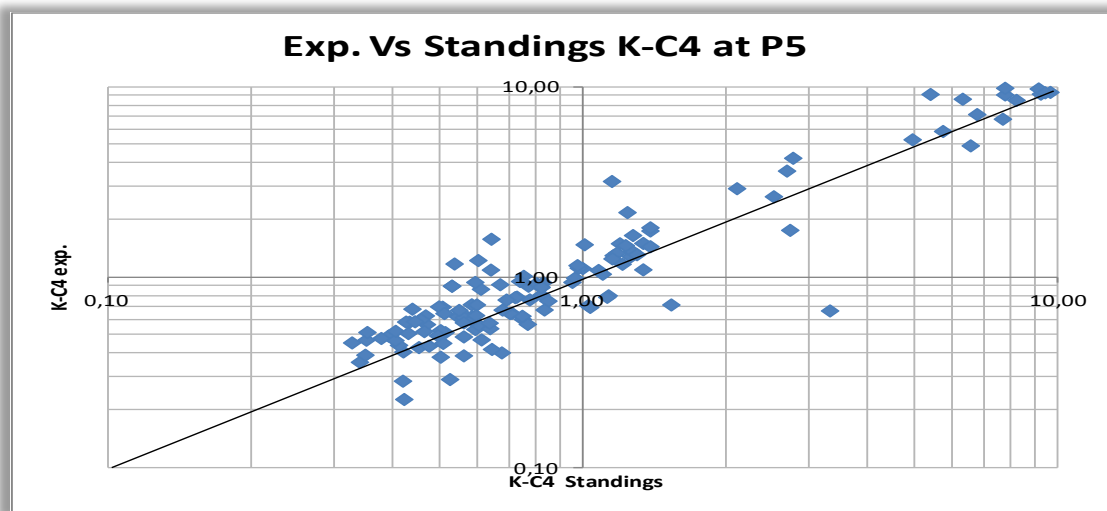


Figure 54: Experimental K-values of C_4H_{10} versus Standing's K-values of C_4H_{10} at P5.

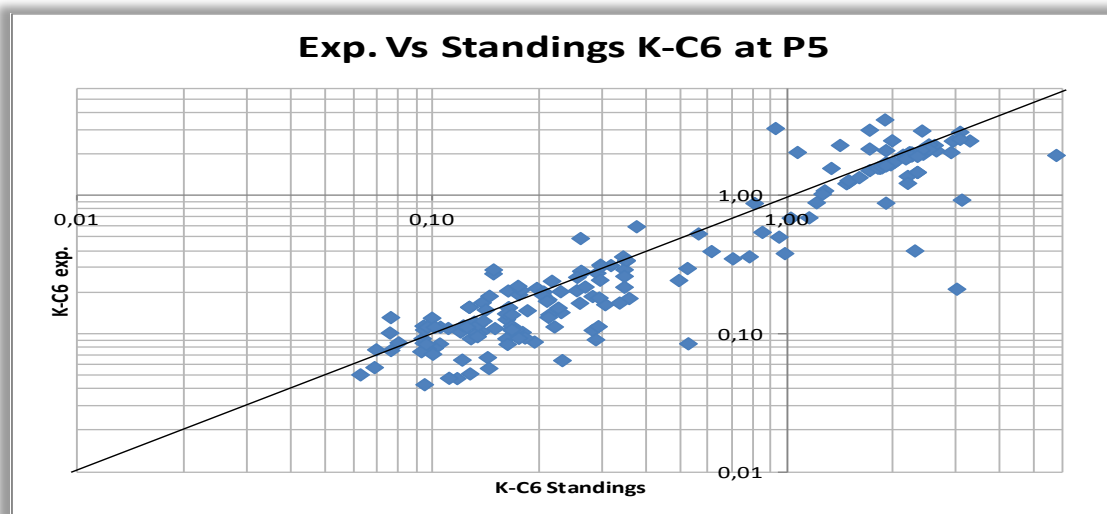


Figure 55: Experimental K-values of C_6H_{12} versus Standing's K-values of C_6H_{12} at P5.

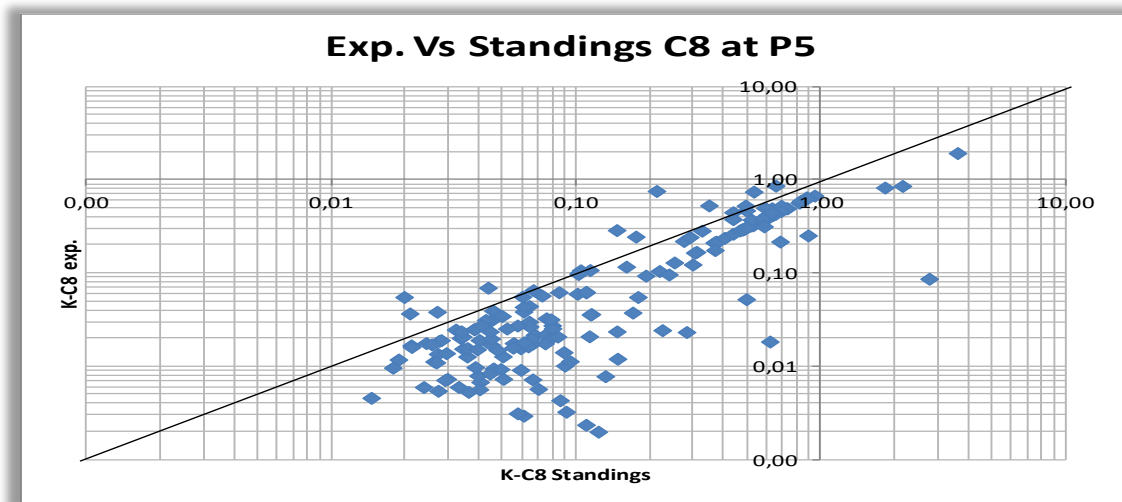


Figure 56: Experimental K-values of C_8H_{14} versus Standing's K-values of C_8H_{14} at P_5 .

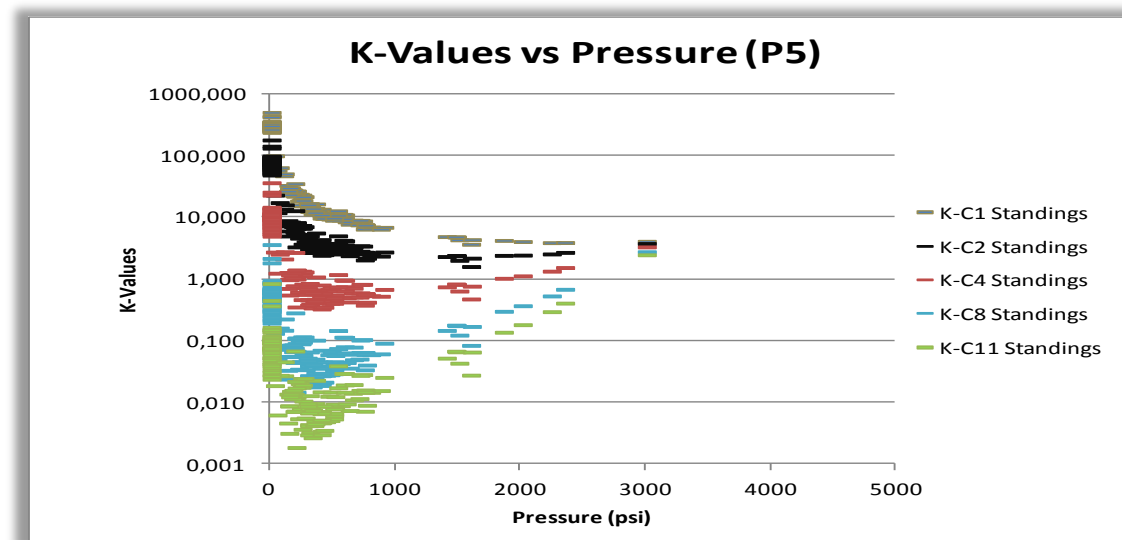


Figure 57: Standing's K-values versus Pressure at P_5 .

As it is observed to the diagrams of the last pressure step the matching between the experimental and the Standing's K-values is satisfying but it is heavily influenced from the mathematical calculation of the liquid compositions. If the compositions were valid, the matching would be for sure better because as mentioned in the sub-chapter 5.3 Standing's K-values follow the experimental at pressures up to 1500 psi and the majority of the 5th DLE pressures are up to this point.